Simple Coupled Midlatitude Climate Models

LYNNE D. TALLEY

Scripps Institution of Oceanography, University of California, San Diego, La Jolla, California

(Manuscript received 23 June 1997, in final form 10 September 1998)

ABSTRACT

A set of simple analytical models is presented and evaluated for interannual to decadal coupled ocean–atmosphere modes at midlatitudes. The atmosphere and ocean are each in Sverdrup balance at these long timescales. The atmosphere's temperature response to heating determines the spatial phase relation between SST and sea level pressure (SLP) anomalies. Vertical advection balancing heating produces high (low) SLP lying east of warm (cold) SST anomalies, as observed in the Antarctic circumpolar wave (ACW), the decadal North Pacific mode, and the interannual North Atlantic mode. Zonal advection in an atmosphere with a rigid lid produces low SLP east of warm SST. However, if an ad hoc equivalent barotropic atmospheric response is assumed, high SLP lies east of warm SST. Relaxation to heating produces behavior like the observed North Atlantic decadal pattern, with low SLP over warm SST. Meridional advection in the atmosphere cannot produce the observed SST/SLP patterns.

The dominant balance in the ocean's temperature equation determines the phase speed of the modes. The coupled mode is nondispersive in all models examined here, indicating the need for additional processes. For modes with an SST–SLP offset as observed in the ACW and North Pacific, Ekman convergence acting as a heat source causes eastward propagation relative to the mean ocean flow. Sverdrup response to Ekman convergence, acting on the mean meridional temperature gradient, causes westward propagation relative to the mean ocean flow. When the ocean temperature adjusts through surface heat flux alone, the mode is advected by the mean ocean flow and is damped.

Relaxation to heating in the atmosphere, when operating with Sverdrup response in the ocean, produces the only complete solution presented here that exhibits growth, with an *e*-folding timescale of order (100 days). This solution appears appropriate for the North Atlantic decadal mode.

In Northern Hemisphere basins, with meridional boundaries, the same sets of dynamics create the observed SST–SLP phase relation. An additional factor is the creation of SST anomalies through variations in the western boundary current strengths, which are related to the zonally integrated wind stress curl over the whole basin. If barotropic and hence fast adjustment is assumed, the resulting positive feedback can maintain or strengthen the coupled anomalies in the North Pacific and interannual North Atlantic modes.

1. Introduction

Interannual and decadal variability in the midlatitude upper ocean and atmosphere has received increased attention in recent years as the time series available for describing such modes have lengthened. The dominant spatial modes of variability in the North Pacific, Pacific–North American (PNA) pattern, and North Atlantic, North Atlantic oscillation (NAO) pattern, with frequency spectra much broader than El Niño were described some time ago, with refinements continuing. An eastward propagating coupled mode in the Southern Ocean has recently been described (White and Peterson 1996), and has a phase relationship between sea surface temperature (SST) and sea level pressure (SLP) anomalies similar to that in the North Pacific decadal mode and the North Atlantic interannual mode (Kushnir and Held 1996) (cartoons in Figs. 1a and 1b). The North Atlantic's decadal mode has a different phase pattern, with low SLP slightly east of warm SST (Kushnir and Held 1996) (cartoon in Fig. 1c).

The general questions for interannual to decadal timescales are whether midlatitude SST anomalies can force the atmosphere directly and locally, as well as being created by anomalous atmospheric forcing (which could well come from the Tropics), and which of several possible mechanisms dominate in creating anomalies in the atmospheric circulation and in the ocean's SST. The well-documented spatial relationships between SST and SLP anomaly centers (reviewed in section 2) are a diagnostic for the validity of various coupled mechanisms. The eastward propagation of the Southern Ocean mode should also be reproduced.

In section 3 various sets of simple, midlatitude coupled ocean and atmosphere mechanisms are investigated

Corresponding author address: Dr. Lynne D. Talley, Scripps Institution of Oceanography 0230, Physical Oceanography Research Division, La Jolla, CA 92093-0230.
E-mail: ltalley@ucsd.edu

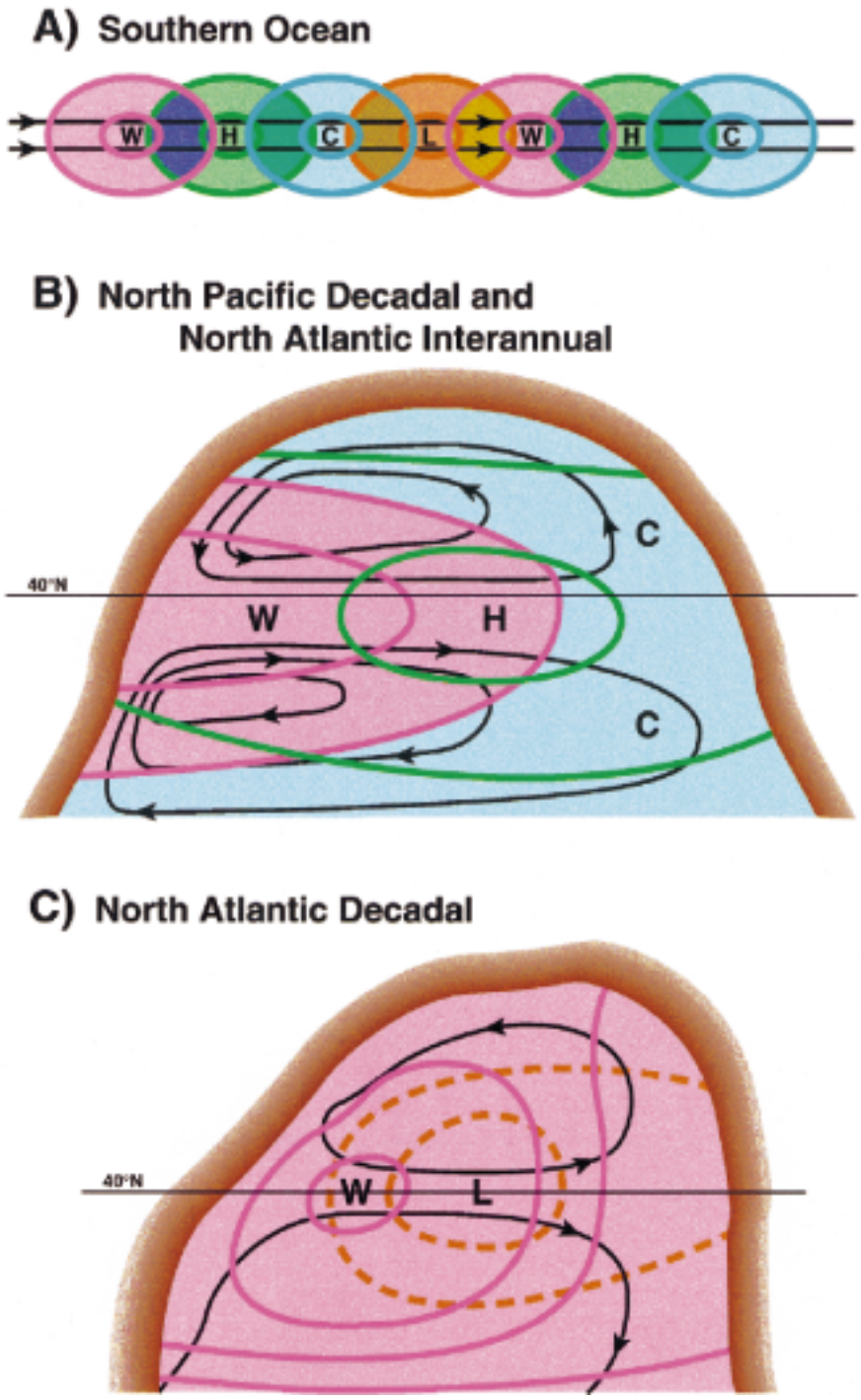

FIG. 1. Schematic of SST and SLP anomalies in the (a) the Southern Ocean, and (b) a Northern Hemisphere (NH) basin, based on White and Peterson (1996) for the Southern Hemisphere (SH) and many sources for the NH (e.g., Tanimoto et al. 1993; Palmer and Sun 1985; Pitcher et al. 1988; Kushnir 1994). The schematic mean ocean circulation is shown in wide black contours (Antarctic Circumpolar Current in the Southern Ocean and subtropical/subpolar gyres in the NH). SST anomalies are shown in red (warm) and blue (cold). SLP anomalies are shown in green (high) and orange (low). The example selected for (b) is high SST in the western boundary region ringed by cold SST, which induces high SLP centered in the basin, and is applicable to the North Pacific decadal and the North Atlantic interannual modes.

to see what kinds of balances can and cannot produce the observed spatial phasing of SST and SLP anomalies. The Antarctic Circumpolar Wave (ACW) and North Pacific decadal and North Atlantic interannual modes appear closest to the solutions of sections 3b(3) and 3c(3). The North Atlantic decadal mode appears to be best described by the solution of section 3e(2). In section 4 the midbasin solution of section 3b(3), which matches the North Pacific decadal SST–SLP pattern, is extended partially to a basin with western and eastern boundaries, and a tendency for positive feedback through barotropic spinup of the circulation is described. These various models should be useful for evaluation of more complex models and observations. They are similar in concept to the equatorial SST mode introduced by Neelin (1991) to describe aspects of El Niño.

2. Background

Gyre-scale sea surface temperature and sea level atmospheric pressure anomaly patterns at short to long timescales have been documented in the midlatitude North Pacific (e.g., Roden and Reid 1961; Davis 1976; Namias et al. 1988; Cayan 1992; Trenberth and Hurrell 1994; Deser and Blackmon 1995; Tanimoto et al. 1993). Most show a high SLP anomaly downstream (east) of a warm SST anomaly, and low SLP east of cold SST, at many timescales. For example, Tanimoto et al. (1993) show that on both short and long timescales (periods shorter than 24 months up to periods longer than 5 years), a warm SST anomaly centered broadly at 40°N, overlying the separated Kuroshio and Oyashio currents (about 35°N and 40°N, respectively) is associated both with cold SST in the eastern and northeastern Pacific and with high SLP shifted eastward and slightly northward relative to the warm SST (Fig. 1b).

The recently described mode of interannual variability for the Southern Ocean, the ''circumpolar wave'' (White and Peterson 1996), shows this same phase relation between SST and SLP anomalies in the 3 to 7 yr band: high SLP centers east of high SST centers (Fig. 1a). The geostrophic wind anomaly is thus poleward over the warm anomalies and equatorward over the cold, which is the same as for the Northern Hemisphere SST–SLP modes described above. The anomalies propagate eastward at a phase speed of about 6–8 cm s^{-1} and also include anomalies of the Antarctic sea ice edge. At a speed of 6 cm s^{-1} at 56°S, they take 12 years to circle the globe and at 8 cm s^{-1}, 9 years. With the observed zonal wavenumber of 2 (see also Qiu and Jin 1997), a warm anomaly appears in a given location every 4 to 6 years. White et al. (1998) show that the SST and SLP anomalies also spiral meridionally, an aspect that is not treated herein.

In the North Atlantic, Palmer and Sun (1985) show warm SST anomalies in the Gulf Stream–North Atlantic Current separation regions associated with high SLP centered to the east and slightly to the north. Kushnir and Held's (1996) composite for interannual variability is similar to this picture, and also includes an SST anomaly of opposite sign (cold) farther to the northeast and an SLP anomaly of opposite sign (low) north of the cold SST anomaly—the pattern which this suggests follows the mean ocean circulation (North Atlantic Current). However, Kushnir and Held's (1996) composite for decadal variability differs from this pattern, with low SLP overlying and slightly east of a warm SST anomaly (Fig. 1c).

In the Northern Hemisphere, the zonal length scale of the coupled mode appears set by the width of the ocean basin. In the Southern Ocean, the mode is zonal wavenumber 2, hence with a wavelength of about 15 000 km (White and Peterson 1996; Qiu and Jin 1997). This may be related to the location of Tasmania/New Zealand and South America/Antarctic Peninsula, which create two subtropical gyres at the latitude of the Antarctic Circumpolar Current (the Pacific gyre and the Atlantic/Indian gyre). Alternatively, internal dynamics related to Rossby waves or instabilities may set the scale. An intrinsic mode of the Southern Hemisphere, the Pacific–South American teleconnection, may also set the spatial scale (e.g., Mo and White 1985; Karoly 1989; Christoph et al. 1998), although this scale may still be related to the disposition of land and ocean.

Observed interannual to decadal atmospheric anomalies appear to be equivalent barotropic (Palmer and Sun 1985; Kushnir and Held 1996). The previously modeled atmospheric anomalies that most resemble the observations are equivalent barotropic except for a significant shift of the surface anomalies to the east (Palmer and Sun 1985; Pitcher et al. 1988).

a. Sea surface temperature anomalies

The maximum SST anomalies associated with the observed climate modes are on the order of 1°C in the Northern Hemisphere (e.g., Miller et al. 1994; Kushnir 1994) and on the order of 0.5°C in the Southern Ocean (e.g., White and Peterson 1996). What sets the location of the maximum anomalies and what are likely maintenance mechanisms? 1) High meridional SST gradients (fronts) are collocated with the SST anomaly centers. Shifting the frontal locations even a small amount results in a stronger SST anomaly than in other latitude bands—the observed temperature change across the Kuroshio is 3°–4°C/1° lat, while across the Antarctic Circumpolar Current fronts the change can be 1°C/1° lat. However, the frontal regions are much narrower meridionally than the anomalous SST regions. 2) Storm tracks overlay the maximum SST gradients. Changes in the strength of the westerlies and vigor of the storms and/or a meridional shift in these patterns could create locally anomalous surface heat flux and mixed layer entrainment and hence SST anomalies. Shifts in the winds also affect the location of maximum Ekman advection, which can thus also result in SST anomalies. 3) In the

Northern Hemisphere, the maximum SST gradient occurs in the general region of western boundary current separation (which is related to the offshore frontal locations). Change in strength of the subtropical and subpolar gyres affects western boundary current transports. A strong subtropical western boundary current creates a warm SST anomaly and a strong subpolar western boundary current creates a cold SST anomaly. Increased strength in both gyres could enhance the meridional SST gradient itself, which could then both be more sensitive to meridional advection and could also enhance baroclinic forcing of the atmosphere.

SST anomalies are driven by the atmosphere, through changes in ocean circulation (e.g., Roden and Reid 1961; Latif and Barnett 1994, 1996) and surface layer properties and flow. Circulation changes include western boundary current strength and separation location, location of the subtropical/subpolar bifurcation in the east, and subduction and advection of anomalies. Subduction and subsurface advection of temperature anomalies around the subtropical gyre as a feedback has been suggested by Latif and Barnett (1994, 1996) and others; such subduction has been documented for the North Pacific by Deser et al. (1996) and Schneider et al. (1998). In the surface layer, stronger westerlies accompanied by enhanced storminess and penetration of storm tracks farther to the east increase heat loss from the ocean mixed layer to the atmosphere and cause deeper ocean mixing, which entrains colder water into the mixed layer (e.g., Cayan 1992; Miller et al. 1994). Ekman transport also changes (e.g., Palmer and Sun 1985). The relative importance of various mechanisms depends on location (Miller et al. 1994).

Subpolar North Pacific patterns of SST and SLP show that cold SST in the Gulf of Alaska region is associated with high SLP (stronger anticyclonic forcing) (Davis 1976; Cayan 1992; Miller et al. 1994). Low SLP in the central Pacific (deep Aleutian Low) spins up the subpolar circulation, advecting more cold water into the separated Oyashio region (Sekine 1988; Hanawa 1995), and warm water northward into the Gulf of Alaska. Chelton and Davis (1982) show increased southward flow in the California Current during high SLP periods. These observations suggest that cold SST in the Gulf of Alaska is due to reduced northward flow of warm water from the subtropics, as also substantiated by changes in bomb-produced tritium inventories in the northern California Current (VanScoy and Druffel 1993).

b. Sea level pressure anomalies

Midlatitude atmospheric SLP anomalies can be created by remote forcing from the Tropics (e.g., Lau and Nath 1996; Graham et al. 1994), and vertical or horizontal advective responses to local heat sources (Smagorinsky 1953), which can be either deep or shallow (e.g., Hoskins and Karoly 1981). The treatment in the following sections includes only local forcing.

At long time and space scales in the atmosphere the Sverdrup balance between vertical stretching and meridional wind holds (Hoskins and Karoly 1981; Palmer and Sun 1985). On the other hand, relative vorticity may become important in the upper troposphere where the mean wind is stronger (W. White and S.-C. Chen 1997, personal communication). The main question here for the atmosphere is the dominant balance in the temperature equation for a given latitude and SST anomaly size, and the associated vertical distribution of heating. Large SST anomalies at midlatitude can force a local response (Pitcher et al. 1988). Midlatitude tropospheric heating at interannual timescales appears to be deep, peaked in midtroposphere (W. White and S.-C. Chen 1997, personal communication). The resulting low-level convergence and vortex stretching create poleward wind over warm SST anomalies through Sverdrup response (Gill 1980), which results in high SLP to the east of high SST (Palmer and Sun 1985) as observed in the ACW and North Pacific (Fig. 1 schematic).

Horizontal advection of atmospheric temperature anomalies also creates a phase shift between SST and SLP anomalies. Whether this creates high or low SLP east of high SST depends on the vertical boundary conditions assumed for the atmosphere (section 3). If, as in Qiu and Jin (1997), it is assumed that the atmosphere is equivalent barotropic (pressure perturbation of the same sign at all heights, and maximum perturbation velocities at the top of the troposphere), then high SLP occurs east of warm SST as observed. If instead the maximum perturbation velocities are at the ground or midtroposphere, then this temperature balance causes low SLP to lie east of high SST (Hoskins and Karoly 1981); in the upper troposphere the pressure anomaly would be of opposite sign.

If atmospheric heating is balanced simply by a thermal damping term with no advection, then the atmosphere temperature anomalies are in phase with SST; thermal wind places maximum wind anomalies over maximum SST gradients, and hence high SLP directly over high SST. This could be the dominant mechanism for the North Atlantic decadal anomalies described by Kushnir and Held (1996).

c. Coupled processes

The number of possible coupled mechanisms is large. The robust phase relation between the midlatitude SST and SLP anomalies suggests that midlatitude models be considered, but external forcing might be necessary to maintain their strength. Peterson and White (1998) show that external forcing for the Southern Ocean anomalies can be provided through teleconnection with the western tropical Pacific. Teleconnection from the western tropical Pacific to the North Pacific through the Hadley circulation has been demonstrated for El Niño timescales

by Tyrell and Karoly (1996), with the downward limb of the Hadley cell forcing atmospheric Rossby waves in the region of the Kuroshio; this could possibly also be a source of SST forcing for this region, or could more generally be the source of changed wind stress curl, which spins up the ocean gyre circulation, thus creating SST anomalies. Lau and Nath (1996) conclude that midlatitude North Pacific anomalies are forced through teleconnections with the tropical Pacific and also show that midlatitude coupled processes can provide positive feedback to maintain the anomalies.

Christoph et al. (1998), in their coupled GCM focused on the Antarctic circumpolar wave, conclude that the Southern Hemisphere Pacific–South American pattern is the most important factor in forcing the ACW, rather than teleconnections tied to El Niño. They suggest that the ACW may not be a true coupled mode, but rather the response of SST in the advective Antarctic Circumpolar Current to a stationary atmospheric pattern.

Simple analytical models incorporating just a few of the possible mechanisms help to isolate possible coupled modes. Predominantly analytical studies of the midlatitude coupled ocean–atmosphere include those of Pedlosky (1975), Palmer and Sun (1985), Liu (1993), Qiu and Jin (1997), White et al. (1998), and Saravanan and McWilliams (1998). The treatment here is most similar to Liu's with respect to various ocean mechanisms. The principal difference here is treatment of the atmosphere's response, which is assumed here to be either in Sverdrup balance (Palmer and Sun 1985) with strongest meridional winds over the strongest SST anomalies or including zonal atmospheric advection of the zonal atmospheric temperature gradient. Pedlosky's (1975) scaled analysis of a similar coupled system emphasizes the finite amplitude feedback instability of a baroclinic wave in the atmosphere, which draws on the heat source of the SST anomalies. SST development is based on ocean Sverdrup transport acting on the meridional temperature gradient for simplicity. A simpler atmosphere is assumed here, and the direct effect of Ekman flow and the weaker effect of zonal temperature gradients are included for the ocean.

Saravanan and McWilliams (1998) use stochastic atmospheric forcing with a preferred length scale and find that combination with advection in a slab ocean sets the timescale, as is the general finding here. Their results depend on the relative strength of zonal advection and heating and on the strength of atmospheric damping compared with the flux between the ocean and atmosphere (as in the comparison of results from sections 3b and 3e below). Their meridional advection mechanism is stochastic and they do not include vertical velocity in the atmosphere in a fundamental way.

Qiu and Jin (1997) used a two-layer quasigeostrophic ocean model with advection of a background meridional temperature gradient by meridional geostrophic flow and zonal advection of temperature anomalies. Because it has two layers, their ocean model admits baroclinically unstable solutions, which dictate the time and hence space scale of the mode. A critical assumption is that the atmosphere is equivalent barotropic, the ramifications of which are explored below in section 3c. Their growing coupled mode has phase-shifted SLP and SST anomalies resulting mainly from eastward advection of the SLP anomaly by the zonal wind.

For Northern Hemisphere basins with gyres of restricted zonal extent, the coupled model of Latif and Barnett (1994, 1996), described above, and the analytical/numerical results of Jin (1997) are relevant. Jin assumed that the atmosphere damps to match the ocean thermal forcing (as in section 3e below); the meridional SST anomalies create zonal wind anomalies, which couple to the ocean through its Sverdrup transport. The ocean includes baroclinic Rossby waves, which provide the important decadal feedback for the closed Northern Hemisphere basin that he explored. When forced by stochastic winds, the ocean response has a broad peak at the basin mode. When coupled to the atmosphere, the decadal response peak is greatly heightened, through positive feedback.

The following section works through various simplified coupled mechanisms for the zonally periodic Southern Ocean. It is possible in this way to eliminate some coupled processes since they do not reproduce the observed phase relations between SST and SLP. The remaining choices can be useful for analyses of coupled numerical models.

3. Simple coupled models for the propagating Antarctic Circumpolar Wave

In both the ACW and the North Pacific decadal mode, a large-scale warm SST anomaly is flanked to the east by a high atmospheric SLP anomaly, and cold SST is flanked to the east by low SLP (schematics in Fig. 1 and references above). Because of the periodicity of these anomalies in the circumpolar wave (zonal wavenumber 2), it is possible to say that these patterns are nearly in quadrature, not just slightly displaced (White and Peterson 1996).

These characteristics are modeled in a simple way here using a quasi-one-dimensional (active zonal variation only) model in both the atmosphere and ocean, with meridional variation confined to a linear background ocean temperature gradient. The ocean model includes SST change through zonal advection by the mean flow, Ekman pumping acting on the upper-layer depth as a proxy for heating, meridional advection due to Sverdrup response to Ekman pumping, and surface heat flux, which in reality depends on wind direction and speed among other factors (e.g., Cayan 1992). Only a very simple approach to ocean heating/cooling is included. Most of these atmosphere and ocean mechanisms are included variously, but not together, in Palmer and Sun (1985), Pedlosky (1975), Liu (1993), and Qiu and Jin (1997).

TABLE 1. Parameters.

Parameter	Function	Magnitude
γ	Ekman pumping effect on ocean temperature	2×10^{-2} K m^{-1}
h_E	Ekman layer thickness	100 m
h_S	Surface velocity relative to Sverdrup flow	500 m
H_A	Troposphere height	10 km
δ	Wind speed relative to wind stress	10 m^2 s kg^{-1}
λ	SST effect on atmospheric heating	4×10^{-6} s^{-1}
ε_1	Surface wind relative to SST amplitude	1×10^{-3} m^2 s^{-3} K^{-1}
r	Atmosphere thermal damping rate	8×10^{-7} s^{-1}
κ	Ocean thermal damping rate	3×10^{-8} s^{-1}
ρ_o	Ocean mean density	1020 kg m^{-3}
$d\overline{T}/dy$	Ocean mean SST gradient	10 K/2000 km
θ_o	Atmosphere mean temperature	250 K
$\partial\theta_o/\partial z$	Atmosphere mean temperature gradient	70 K/10 km
$\overline{u}_A$	Atmosphere mean zonal wind	10 m s^{-1}

The atmosphere here is heated and cooled directly above the temperature anomalies with maximum heating at midtroposphere. Clearly the actual heating distribution has a more complicated vertical structure, but as long as the maximum heating is not at the ground, this choice provides the simplest framework for the basic physics in the lower troposphere. Four atmospheric responses to midlevel heating anomalies are considered: 1) vertical advection giving rise to a Sverdrup response similar to the tropical model of Gill (1980), 2) zonal advection of the anomalous temperature, 3) meridional advection of the anomalous temperature, and 4) relaxation to the heating source. Vertical advection (adiabatic heating) leads easily to the observed offset between the SST and SLP anomalies in the ACW, while neither atmospheric relaxation nor meridional advection can. Atmospheric relaxation is the most likely response for the North Atlantic decadal mode based on its different SST–SLP phase structure. For simplicity, it is assumed that response to warm and cold anomalies is of similar magnitude but opposite effect although an asymmetric response is seen in Pitcher et al. (1988).

Further elaborations of this model, not considered here, rapidly become complex, involving, for instance, propagation of Rossby waves in both the ocean and atmosphere at differing phase speeds, the major variations in mixed layer depth across the Antarctic Circumpolar Current or Kuroshio/Gulf Stream, variations in the meridional ocean temperature gradient, subduction and subsurface westward advection of temperature anomalies in the confined subtropical gyres north of the ACC along with sea surface propagation through subpolar gyres south of the ACC, etc. Eddy fluxes and storm tracks in the atmosphere are not considered explicitly here—the vorticity balance is shown to be dominated by the Sverdrup balance for these long time and space scales, and the effect of eddy fluxes in the temperature equation is parameterized as Newtonian cooling.

a. Ocean and atmosphere model formulations

The modeled ocean consists of a single layer of uniform depth, representing the ocean's mixed layer. Simple vertical structure is permitted in the troposphere in order to calculate the vertical stretching and to check the appearance of baroclinicity, which can be compared with observations. The simplest model geometry is periodic in the zonal (x) direction and assumes no meridional (y) dependence—hence is one-dimensional in the zonal direction. The next simplest geometry, with a degree of two-dimensionality, includes a linear background meridional temperature gradient in the ocean. The large collection of parameters endemic to even an idealized coupled model is listed in Table 1 with units and a brief description of their function. Many different balances in the atmosphere and ocean are explored with results summarized in Table 2.

1) OCEAN MODEL

Assume that the sea surface temperature and zonal and meridional velocities are composed of a background state and an anomaly:

$$T(x, y, t) = \overline{T}(y) + T'(x, y, t)$$
$$u(x, y, t) = \overline{u} + u'(x, y, t)$$
$$v(x, y, t) = v'(x, y, t), \qquad (1a–c)$$

where $\overline{T}$ and $\overline{u}$ are the background SST and zonal velocity and T', u', and v' are the modeled anomalies. Temperature evolves according to

$$\frac{\partial T'}{\partial t} = (\overline{u} + u')\frac{\partial T'}{\partial x} + v'\frac{\partial \overline{T}}{\partial y} = -\gamma w_E - \kappa T', \quad (2)$$

where $-\kappa T'$ is the anomalous surface heat flux, which damps the anomaly to zero. The Ekman pumping w_E arises from the curl of the wind stress, $\boldsymbol{\tau}$; γ is a positive, empirical constant (with units °C m^{-1}) and is like the upper layer's mean vertical temperature derivative $\partial\overline{T}/\partial z$. This Ekman pumping forcing of SST increases SST in the near-surface thermocline in regions of convergence and downwelling, and decreases SST in regions of divergence/upwelling. Such a response to vertical advection, but also inversely proportional to the changing surface layer depth (which here is constant), is often used

TABLE 2. Coupled mode behaviors.

	Atmosphere			
Ocean	Vertical advection $w\ (\partial\overline{\theta}/\partial z) = Q_A$	Zonal advection $u_A\ (\partial\theta/\partial x) = Q_A$	Zonal advection, assuming equivalent barotropic $u_A\ (\partial\theta/\partial x) = Q_A$	Temperature relaxation $0 = Q_A - r\theta$
Ekman pumping $\partial T'/\partial t + \overline{u}(\partial T'/\partial x) = -\gamma w_E$	SLP high downstream of SST high	SLP low downstream of SST high	SLP high downstream of SST high	SLP low over SST high
	Baroclinic atmosphere	Baroclinic atmosphere	Equivalent BT atmosphere	Baroclinic atmosphere
	Eastward propagation relative to mean ocean flow	Westward propagation relative to mean ocean flow	Eastward propagation relative to mean ocean flow	Advected with the mean ocean flow
				Damped due to atmosphere relaxation
Surface heat flux $\partial T'/\partial t + \overline{u}(\partial T'/\partial x) = -\kappa T'$	SLP high downstream of SST high	SLP low downstream of SST high	SLP high downstream of SST high	SLP low over SST high
	Baroclinic atmosphere	Baroclinic atmosphere	Equivalent BT atmosphere	Baroclinic atmosphere
	Advected with the mean ocean flow	Advected with the mean ocean flow	Advected with the mean ocean flow	Advected with the mean ocean flow
	Damped due to ocean	Damped due to ocean	Damped due to ocean	Damped due to ocean
Sverdrup response and surface heat flux $\partial T'/\partial t + \overline{u}(\partial T'/\partial x) = -v_s(d\overline{T}/dy) - \kappa T'$	SLP high downstream of SST high	SLP low downstream of SST high	SLP high downstream of SST high	SLP low over SST high
	Baroclinic atmosphere	Baroclinic atmosphere	Equivalent BT atmosphere	Baroclinic atmosphere
	Westward propagation relative to mean ocean flow	Eastward propagation relative to mean ocean flow	Westward propagation relative to mean ocean flow	Advected with the mean ocean flow
	Damped due to ocean	Damped due to ocean	Damped due to ocean	Damped due to ocean
				Growth due to atmosphere relaxation

in tropical ocean models (e.g., Zebiak and Cane 1987; Clement et al. 1996). However, this mechanism does not appear to be dominant in upper-ocean response in midlatitudes (Miller and Schneider 1998). Instead, a Sverdrup response, included below in Eqs. (6)–(8) is likely the most important means for changing SST in respose to the wind.

The uniform background surface velocity $\overline{u}$ is taken to be the average geostrophic eastward speed of the Antarctic Circumpolar Current. The surface velocity anomaly u' has a thermal wind and an Ekman part:

$$u'(x, y, t) = u'_g(x, y, t) + u'_E(x, y, t) = -\frac{g\alpha}{f\rho_o}\int_0^h \frac{\partial T'}{\partial y}dz + \frac{\tau^{(y)}}{f\rho_o h_E}, \quad (3)$$

where α is the thermal expansion coefficient and h is the constant thickness of the layer containing the temperature anomaly; ρ_o is the constant background density, f is the Coriolis parameter, u'_E is the Ekman flow associated with the anomalous meridional wind stress, and h_E is the Ekman layer thickness, which in the simplest model could be chosen equal to h. The thermal wind portion is zero throughout since the background meridional temperature gradient is assumed to be either zero (concentration on Ekman pumping response) or constant (concentration on Sverdrup advection response), so no mean gradient in T' develops. Hence only the Ekman portion of u' contributes to the anomaly development in this simple model.

The Ekman pumping w_E for (2) is

$$w_E = \mathbf{k}\cdot\boldsymbol{\nabla}\times\frac{\boldsymbol{\tau}}{\rho_o f} = \frac{1}{\rho_o f}\left(\frac{\partial\tau^{(y)}}{\partial x} - \frac{\partial\tau^{(x)}}{\partial y} + \frac{\beta(\overline{\tau}^{(x)} + \tau^{(x)})}{f}\right), \quad (4)$$

where β is the meridional derivative of f. The wind stress is assumed to have a steady, uniform zonal mean component and both meridional and zonal anomalies:

$$\boldsymbol{\tau} = \overline{\boldsymbol{\tau}} + \boldsymbol{\tau}'(x, t) = \mathbf{i}[\overline{\tau}^{(x)} + \tau^{(x)}(x, y, t)] + \mathbf{j}\tau^{(y)}(x, y, t). \quad (5)$$

The ocean's anomalous meridional velocity is important when there is a background temperature gradient. The surface velocity has geostrophic and Ekman components:

$$\boldsymbol{v}'(x,y,t) = \boldsymbol{v}'_g + \boldsymbol{v}'_E = \frac{g\alpha}{f\rho_o}\int_0^h \frac{\partial T'}{\partial x}dz - \frac{\tau^{(x)}}{f\rho_o h_E}. \quad (6)$$

The planetary geostrophic balance is assumed for the ocean:

$$\beta v'_g = f\frac{\partial w}{\partial z}. \quad (7)$$

When this is integrated vertically, the geostrophic portion of (6) is considered to arise from Sverdrup balance:

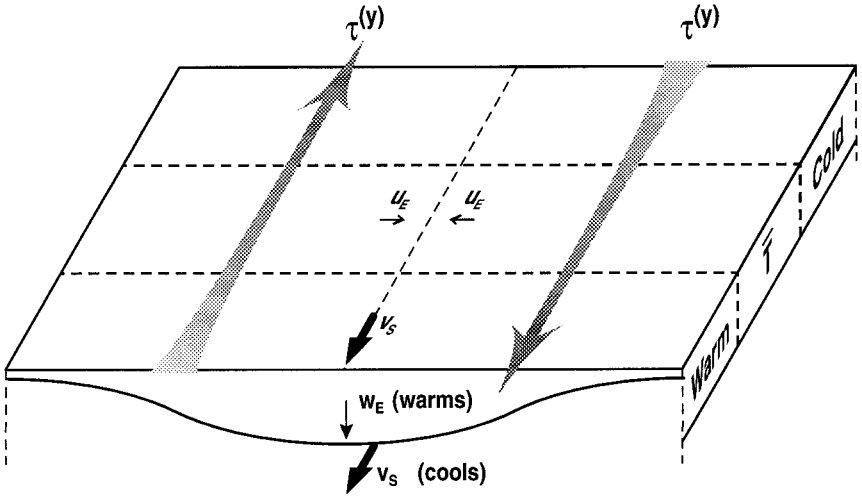

FIG. 2. Ocean response to meridional wind anomaly pattern, with a mean meridional temperature gradient. The diagram is appropriate for the NH; the warming and cooling tendencies are correct for the SH as well. The wind causes zonal Ekman transport u_E convergence, which causes Ekman pumping w_E and hence meridional Sverdrup transport v_S. Ekman pumping in some models is a proxy for heat convergence (downwelling–warming) and divergence (upwelling–cooling). Sverdrup transport acts on the mean temperature gradient. These two effects oppose each other. The Sverdrup transport mechanism is the more likely physically.

$$v_g' = \frac{1}{h_S}\frac{f}{\beta}w_E. \tag{8}$$

Here h_S has units of meters and relates the surface velocity to the Sverdrup transport and thus depends on how the latter is distributed vertically; it is not the depth of an actual layer. All advective changes in SST in (2) occur through Ekman pumping, illustrated in Fig. 2. In Ekman convergence regions, where $w_E < 0$, the pumping term on the right side of (2) yields warming (Fig. 2 vertical velocity). On the other hand, Sverdrup response to the same downward Ekman pumping is equatorward flow, which, when it acts on the mean meridional temperature gradient, yields cooling (Fig. 2 meridional velocity).

2) ATMOSPHERE MODEL

The atmosphere acts on the ocean through anomalous heat flux and through wind anomalies, assumed to be geostrophic and in thermal wind balance. The wind is assumed to have a zonal mean, $\overline{u}_A$, and zonal and meridional anomalies, u_A and v_A. The meridional wind anomaly v_A is geostrophic:

$$fv_A = \frac{1}{\rho_A}\frac{\partial p_A}{\partial x} \quad \text{and} \quad \frac{\partial v_A}{\partial z} = \frac{g}{f\theta_o}\frac{\partial \theta'}{\partial x}, \tag{9a,b}$$

where p_A is the pressure, ρ_A is the mean density, and θ' and θ_o are the potential temperature anomaly [see (14) below] and mean, making the Boussinesq approximation. The wind velocity is assumed to be proportional to the wind stress:

$$v_A = \delta\tau^{(y)}, \tag{10}$$

where δ has units of m^2 s kg^{-1} and is constant. The linear, quasigeostrophic vorticity equation for the atmosphere is assumed:

$$\frac{\partial \zeta_A}{\partial t} + u_A\frac{\partial \zeta_A}{\partial x} + \beta v_A = f\frac{\partial w_A}{\partial z}, \tag{11}$$

where the relative vorticity is

$$\zeta_A = \frac{\partial v_A}{\partial x} - \frac{\partial u_A}{\partial y}.$$

For quasigeostrophy, the Rossby number, U/fL, and the aspect ratio, H/L, are small, where U, H, and L are characteristic scales for the circumpolar wave. These assumptions are clearly satisfied for any reasonable wind speed with length scale of 6000 km, yielding a Rossby number of order 0.01.

The timescale of the coupled mode is several years. This is much longer than the timescale of atmospheric Rossby waves, for which the first two terms in (11) are important. The zonal length scale is large. Thus the nondimensional parameters $\beta L^2/U$ and βLT are large, where T is the characteristic timescale. [For length scales of order 6000 km (half wavelength of the circumpolar wave), wind speeds of 10 m s^{-1}, and timescales of several years, $\beta L^2/U = O(50)$; $\beta LT = O(5000)$.] The atmosphere's vorticity balance thus reduces to the steady, linear Sverdrup balance:

$$\beta v_A = f\frac{\partial w_A}{\partial z}, \tag{12}$$

which is the analog to (7) for the ocean. Balance (12) was used by Gill (1980) for the Tropics, and by Hoskins and Karoly (1981) and Palmer and Sun (1985).

The potential temperature equation for the atmosphere with a heating source and linear damping is

$$\frac{\partial \theta'}{\partial t} + \overline{u}_A \frac{\partial \theta'}{\partial x} + v_A \frac{\partial \overline{\theta}}{\partial y} + w_A \frac{\partial \overline{\theta}}{\partial z} = Q_A(x, y, z, t) - r\theta', \tag{13}$$

where the potential temperature consists of a mean and an anomaly:

$$\theta(x, y, z, t) = \theta_o + \overline{\theta}(y, z) + \theta'(x, y, z, t). \tag{14}$$

Equation (13) is linearized about the zonal mean wind $\overline{u}_A(z)$; Q_A is a source of potential temperature (heating). It is chosen to be proportional to the SST anomaly and maximum well above the ground:

$$\begin{aligned} Q_A &= Q_o(x, y, t) \sin(\pi z/H_A) \\ &= \lambda T'(x, y, t) \sin(\pi z/H_A), \end{aligned} \tag{15}$$

where H_A is chosen here to be 10 km, the height of the tropopause, and λ is a positive constant (with units of s^{-1}). Smagorinsky's (1953) heating function choice was similar to (15) and also included exponential dependence, which allowed the maximum heating height to vary. A very simple form is used here since the emphasis is on the surface wind and the process that creates its direction. This is insensitive to the height of maximum heating.

Scaling of the atmosphere's temperature equation (13) was discussed by Hoskins and Karoly (1981). Assuming a timescale of 3 yr, temperature anomaly of 1 K, mean zonal wind of 10 m s^{-1}, anomalous meridional wind of 1 m s^{-1}, vertical velocity of 10^{-4} m s^{-1} based on (12), meridional temperature gradient of 10 K/5000 km, and vertical temperature gradient of 10 K/5 km, the time-dependent term in (13) is order 20 times smaller than vertical advection, and the two horizontal advection terms are order 7–10 times larger than vertical advection. There is likely partial cancellation of the horizontal advection terms, so the seemingly larger magnitude of these individual terms compared with vertical advection might not hold. Hence vertical advection can also be considered in dominant balances.

Boundary conditions for the atmosphere must be imposed to obtain solutions. The most straightforward assume rigid boundaries at the ground and tropopause:

$$w_A = 0 \quad \text{at } z = 0, H_A. \tag{16}$$

In the following subsections various simplifications of the ocean (2) and atmosphere (13) temperature equations isolate different processes in each that lead to the observed spatial phasing of SST and SLP anomalies. Results are summarized in Table 2. It will be seen that the choice of atmospheric process determines the SST–SLP relation. Eastward and westward phase propagation directions are also determined for each combination of processes, and are found to depend largely on the choice of ocean process since time dependence resides in the ocean temperature equation. Clearly the actual solutions include all of the terms to some degree. The subsections are organized according to which atmospheric process is assumed dominant (columns of Table 2); several ocean processes are considered within each subsection (rows of Table 2).

Based on the SST–SLP pattern in the many solutions presented below, the most relevant solutions are section 3b(3) and possibly 3c(3) for the ACW and North Pacific decadal and North Atlantic interannual modes, and section 3e(2) for the North Atlantic decadal mode. Ocean damping can be included in any of these solutions and just causes decay.

b. Atmosphere: Vertical advection balancing heating

The first choice for a dominant balance in the atmosphere's temperature equation (13) is between vertical advection and heating:

$$\begin{aligned} w_A(x, y, z)\frac{\partial \overline{\theta}}{\partial z} \equiv w_A \frac{\theta_o}{g} N^2 &= Q_A(x, y, z, t) \\ &= \lambda T'(x, y, t) \sin(\pi z/H_A). \end{aligned} \tag{17}$$

The vertical velocity anomaly is upward in heating and downward in cooling regions. It satisfies the boundary conditions (16). (Note that only anomalies are considered, so symmetry of heating and cooling really means symmetry in the degree of local atmospheric heating about the mean.) The atmosphere's vorticity equation (12) yields

$$\begin{aligned} v_A &= \frac{f}{\beta}\frac{\partial w_A}{\partial z} = \frac{f}{\beta} G_1 \lambda T'(x, y) \cos(\pi z/H_A) \\ G_1 &= \frac{g}{\theta_o N^2}\frac{\pi}{H_A}, \end{aligned} \tag{18a,b}$$

where N^2 is assumed constant. The meridional wind at the ground is thus poleward over warm SST and equatorward over cold SST (Fig. 3a) as was found by Gill (1980) for his tropical solutions, and by White et al. (1998) for solutions pertaining to the circumpolar wave. Above $z = H_A/2$, the meridional wind and SLP anomaly signs reverse. The vertical structure is baroclinic rather than equivalent barotropic, but does have the observed spatial SLP–SST phasing in the lower troposphere.

The meridional wind anomalies cause Ekman pumping (4), which then acts on the SST, through either upper-layer heat convergence (one-dimensional solution) or Sverdrup advection of the mean temperature gradient (quasi-two-dimensional solution), as described next. Damping of the ocean's SST anomaly through the heating term can be included throughout without modifying the effect of these two basic mechanisms.

1) OCEAN UPPER-LAYER HEAT CONVERGENCE (TABLE 2, ROW 1, COLUMN 1)

Assume for simplicity that the mean ocean temperature is uniform ($d\overline{T}/dy = 0$). Then SST evolution (2) becomes

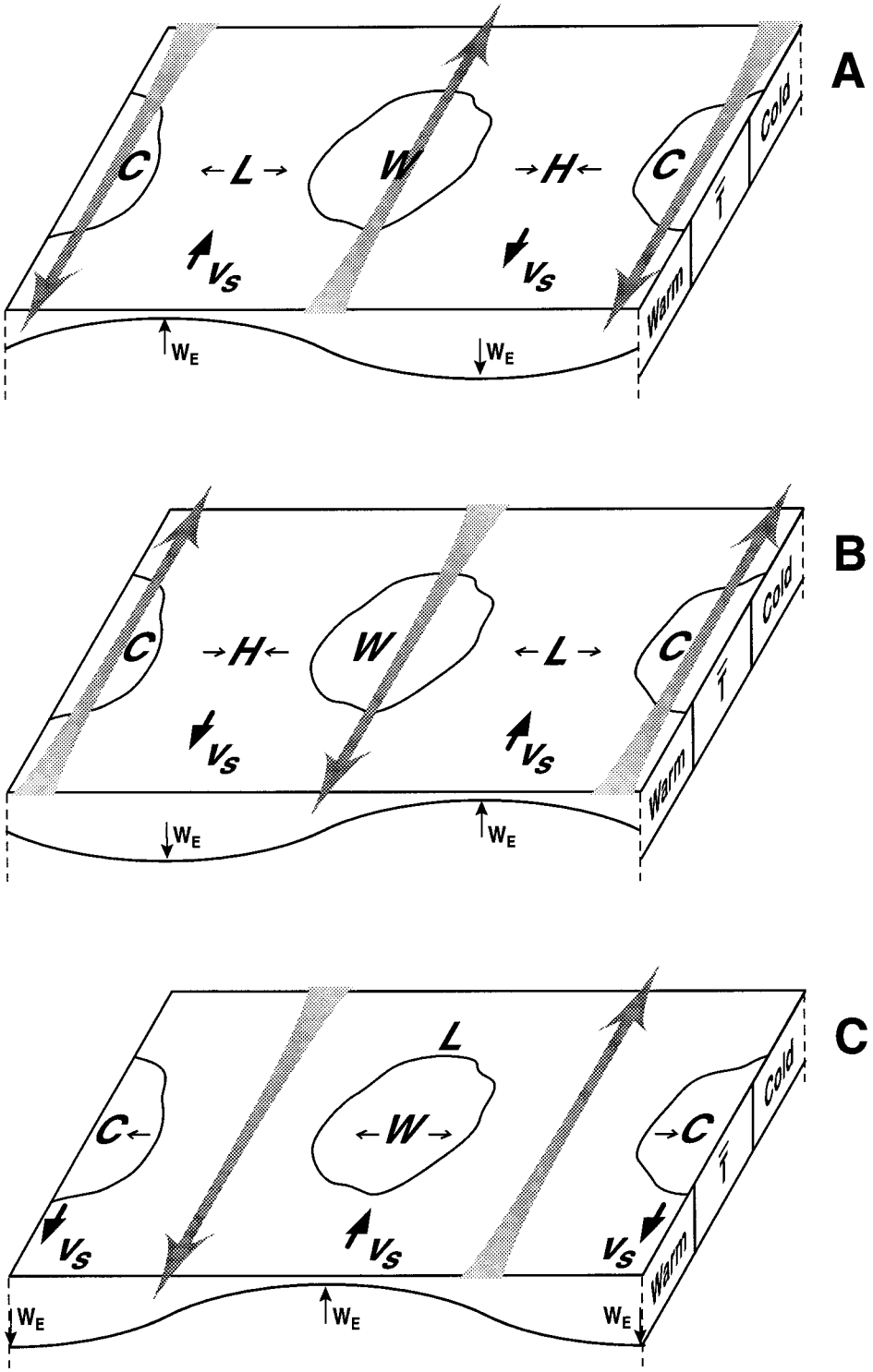

FIG. 3. Meridional wind anomaly $\tau^{(y)}$ (gray arrows), Ekman transport u_E (thin zonal arrows), Ekman pumping w_E, and Sverdrup transport v_S superimposed on schematic warm (W) and cold (C) SST anomalies and a mean meridional ocean temperature gradient. (a) Assuming vertical advection balancing heating in the atmosphere (Table 2, column 1) and also zonal advection balancing heating in the atmosphere with an ad hoc equivalent barotropic assumption (Table 2, column 3). This might be the best balance for the ACW and the North Pacific decadal and North Atlantic interannual modes. (b) Assuming zonal advection balancing heating in the atmosphere with rigid-lid boundary conditions (Table 2, column 2). (c) Assuming relaxation of atmospheric temperature to local heating (Table 2, column 4).

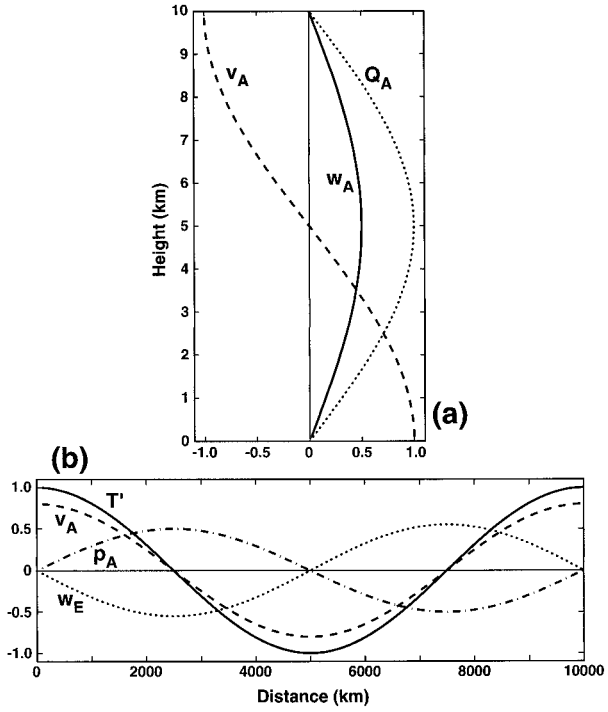

FIG. 4. Solution for vertical advection balancing heating in the atmosphere. Of the solutions presented here, this is the most likely for the ACW and the North Pacific decadal and the North Atlantic interannual modes. (See Fig. 9 for further elaboration on the North Pacific mode.) Units are arbitrary. (a) Heating Q_A, vertical velocity w_A, and meridional wind v_A with signs appropriate directly above a maximum positive SST anomaly. (b) Anomalies of SST T', SLP p_A, meridional surface wind v_A, and Ekman pumping w_E. Positive w_E (upwelling) cools SST directly, while poleward Sverdrup flow in the same location warms SST.

$$\frac{\partial T'}{\partial t} + [\overline{u} + u_{ev} + u_E(x, t)]\frac{\partial T'}{\partial x} = 0, \qquad (19)$$

where

$$u_{ev} = G_1\frac{\gamma\lambda}{\rho_o\delta\beta} \quad \text{and} \quad u_E = \frac{\tau^{(y)}}{f\rho_o h_E} = G_1\frac{\lambda}{\rho_o\delta\beta h_E}T'. \qquad (20a,b)$$

Advection by the uniform background flow $\overline{u}$ is augmented by the positive definite u_{ev}, which arises from the Ekman pumping term in (2). As a reminder, the positive parameter γ is the proportionality factor between Ekman pumping and SST anomaly (2), δ relates wind speed to wind stress (10), and λ relates vertical velocity in the atmosphere to the SST anomaly T' (15).

Zonal Ekman advection $u_E(x, t)$ arising from the meridional wind stress anomalies creates a nonlinearity and hence shocks on the east side of the warm anomalies. In the presence of diffusion (not included), this produces a form of Burger's equation, where the shock width depends on diffusivity and propagation speed. Since the zonal temperature gradient does not feed back into the meridional wind [e.g., Eq. (18)], the presence of the shocks is interesting but not important to this simple model and is hence ignored.

A zonally periodic solution to (19) relevant to the circumpolar wave, ignoring $u_E(x, t)$, is

$$T' = T_o\cos(kx - \omega t). \qquad (21)$$

The frequency and zonal wavelength are related nondispersively through

$$\omega = k(\overline{u} + u_{ev}). \qquad (22)$$

The associated anomalies of geostrophic meridional wind velocity (18), sea level atmospheric pressure (9a), and ocean Ekman pumping (4) are

$$v_A(z = 0) = G_1\frac{f}{\beta}\lambda T_o\cos(kx - \omega t) \qquad (23a)$$

$$p_A(z = 0) = G_1\frac{f^2\rho_A}{\beta}\frac{\lambda T_o}{k}\sin(kx - \omega t) \qquad (23b)$$

$$w_E = -G_1\frac{\lambda}{\rho_o\delta\beta}kT_o\sin(kx - \omega t). \qquad (23c)$$

These are illustrated in Figs. 3a and 4 for the Northern Hemisphere ($f > 0$). Note that the surface wind stress is poleward over warm anomalies, atmospheric pressure is high east of a warm anomaly, and Ekman pumping is downward (negative) under the high pressure. The time- and space scales of the coupled mode are related by (22) and must be set externally. The scales and speeds are discussed in section 3f.

In this solution, regardless of the ocean model, the relative phase of the temperature, pressure, and wind stress anomalies at the ground in the Southern Hemisphere matches the east–west phasing of White and Peterson's (1996) circumpolar wave and the dominant interannual surface patterns in the Northern Hemisphere and decadal pattern in the North Pacific (e.g., Tanimoto et al. 1993; Palmer and Sun 1985; Kushnir 1994), although the continental boundaries complicate the Northern Hemisphere zonal propagation, as discussed below in section 4. However, because this model includes a reversal of meridional winds and change in sign of the pressure anomaly above the midtroposphere heating source (15), it does not match the observations, which suggest equivalent barotropic behavior. [It has been suggested (W. White and S. -C. Chen 1997, personal communication) that relative vorticity in the upper troposphere, which may become important because the mean wind is so strong there, can alter these vertical advective/heating solutions so that they appear to be equivalent barotropic.]

With the SST anomaly set by surface layer heat convergence and divergence, the coupled mode (21)–(23) propagates eastward relative to the mean ocean flow. Using the parameters of Table 3, the phase speed is about 4 cm s^{-1} (see section 3f).

TABLE 3. Estimated zonal phase propagation speeds relative to mean ocean speed.

Model	Phase speed	Phase speed (cm s^{-1})
Vertical advection; Ekman response	$u_{ev} = G_1 \frac{\gamma\lambda}{\rho_o \delta \beta}$	4
Vertical advection; Sverdrup response	$u_{\mathrm{Sv}} = G_1 \frac{f}{\beta^2} \frac{\lambda}{\rho_o \delta h_S} \frac{d\overline{T}}{dy}$	−18
Zonal advection, rigid-lid; Ekman response	$u_{ez} = -G_2 \frac{\gamma}{\rho_o \delta} \frac{\lambda}{f^2 \overline{u}_A}$	−1
Zonal advection, rigid-lid; Sverdrup response	$u_{sz} = -G_2 \frac{\lambda}{f \overline{u}_A} \frac{1}{\rho_o \delta \beta h_S} \frac{d\overline{T}}{dy}$	5
Zonal advection, equivalent barotropic; Ekman response	$u_{ezbt} = \frac{\gamma \epsilon_1}{\rho_o \delta f^2 \overline{u}_A}$	2
Zonal advection, equivalent barotropic; Sverdrup response	$u_{szbt} = \frac{\epsilon_1}{\rho_o f \overline{u}_A \beta \delta h_S} \frac{d\overline{T}}{dy}$	−10
	Decay rate	Decay rate (s^{-1})
Atmosphere relaxation; Ekman response; damping	$\kappa + k^2 G_3$	6×10^{-8} (10 000 km wavelength)
Atmosphere relaxation; Sverdrup response; damping	$\kappa - k^2 G_4$	-1×10^{-7} (10 000 km wavelength)

2) OCEAN SURFACE HEAT FLUX (TABLE 2, COLUMN 1, ROW 2)

If the ocean changes only through heating and cooling rather than Ekman pumping and vertical advection is still the dominant process balancing atmospheric heating, the ocean temperature balance (2) is

$$\frac{\partial T'}{\partial t} + \overline{u} \frac{\partial T'}{\partial x} = -\kappa T', \tag{24}$$

where warm anomalies cool (and the atmosphere above heats) and the opposite. This simply damps the anomalies:

$$T' = T_o e^{-\kappa t} \cos[k(x - \overline{u}t)] \tag{25a}$$

$$v_A(z = 0) = G_1 \frac{f}{\beta} \lambda T_o e^{-\kappa t} \cos[k(x - \overline{u}t)] \tag{25b}$$

$$p_A(z = 0) = G_1 \frac{f^2}{\beta} \frac{\rho_A \lambda}{k} T_o e^{-\kappa t} \sin[k(x - \overline{u}t)]. \tag{25c}$$

The signal is advected with the mean ocean velocity. The meridional wind is still proportional to T' and hence high pressure lies east of warm SST, which matches observations. This behavior will be included in all of the remaining solutions without further comment.

3) OCEAN SVERDRUP ADVECTIVE RESPONSE (TABLE 2, COLUMN 1, ROW 3)

If the mean ocean temperature gradient, which is equatorward almost everywhere, is included, then the equatorward (poleward) Sverdrup flow (8) caused by Ekman downwelling (upwelling) can also create SST anomalies. The effect of this Sverdrup advection mechanism on the coupled mode propagation is of opposite sign to the mixed layer heat convergence mechanism, which was just explored in (19)–(23) (Fig. 2).

Assume that the background meridional temperature gradient $d\overline{T}/dy$ is constant. The problem is then pseudo-one-dimensional, with T' and v' independent of y and $u' = 0$. Using (8) with (4) and (10) for the meridional advection term in (2), and now also including the ocean surface flux term κ proportional to temperature, which damps the SST anomalies, we have

$$\frac{\partial T'}{\partial t} + \overline{u} \frac{\partial T'}{\partial x} = -G_1 \frac{f}{\beta} \frac{\lambda}{\rho_o \delta \beta h_s} \frac{d\overline{T}}{dy} \frac{\partial T'}{\partial x} - \kappa T', \tag{26}$$

where G_1, defined in (18b), is positive. Assuming again a zonally periodic solution, the anomalies are

$$T' = T_o e^{-\kappa t} \cos[k(x - (\overline{u} + u_{\mathrm{Sv}})t)] \tag{27a}$$

$$v_A = G_1 \frac{f}{\beta} \lambda T_o e^{-\kappa t} \cos[k(x - (\overline{u} + u_{\mathrm{Sv}})t)] \tag{27b}$$

$$p_A = G_1 \frac{f^2}{\beta} \frac{\rho_A \lambda}{k} T_o e^{-\kappa t} \sin[k(x - (\overline{u} + u_{\mathrm{Sv}})t)] \tag{27c}$$

$$v_g = -G_1 \frac{f}{\beta^2} \frac{\lambda}{\rho_o \delta h_s} k T_o e^{-\kappa t} \sin[k(x - (\overline{u} + u_{\mathrm{Sv}})t)] \tag{27d}$$

$$u_{\mathrm{Sv}} = G_1 \frac{f}{\beta^2} \frac{\lambda}{\rho_o \delta h_s} \frac{d\overline{T}}{dy}. \tag{27e}$$

The solution is identical to (23) except for the phase speed and inclusion of damping and is illustrated in Figs.

3a and 4, using the Sverdrup response arrows. The wind remains poleward over warm and equatorward over cold SST anomalies. This creates Ekman pumping (suction) and equatorward (poleward) ocean Sverdrup transport east of warm (cold) SST. This advects cold (warm) water into the ocean east of warm (cold) SST anomalies. Therefore the mode propagates westward relative to the mean ocean flow $\overline{u}$ since u_{sv} is negative for both the Southern and Northern Hemispheres. The phase speed is -18 cm s^{-1} for the parameters chosen in Table 3 (section 3f).

If the initial conditions were truly two-dimensional, with temperature anomalies limited in the meridional direction, then there would also be anomalous zonal winds giving rise to meridional Ekman flow, v'_E. If the temperature anomalies were symmetric in the north–south direction and the background meridional temperature gradient uniform (both of which are fairly reasonable first-order assumptions), the meridional Ekman advection would accomplish two things: pumping under high pressure and suction under low, as already modeled above, and strengthening the meridional gradient of T' under high pressure regions and weakening it in the low pressure regions. That is, it would be frontogenetic under highs and frontolytic under lows. This might have some effect on the atmospheric circulation, but it likely would not be as important as a simple advection of warm or cold water.

c. Atmosphere: Zonal advection balancing heating

Next is considered separately the result of balancing heating in the atmosphere by zonal advection in (13):

$$\overline{u}_A \frac{\partial \theta'}{\partial x} = \overline{u}_A \frac{f\theta_o}{g}\frac{\partial v_A}{\partial z} = Q_A = \lambda T' \sin(\pi z/H_A) \quad (28)$$

using thermal wind (9). If the zonal mean wind $\overline{u}_A$ is uniform and heating is chosen as in (15), (28) yields

$$v_A = V_o(x, y, t) - G_2 \frac{\lambda}{f\overline{u}_A} T'(x, y, t) \cos(\pi z/H_A)$$

$$w_A = W_o + V_o z - G_2 \frac{H_A}{\pi}\frac{\lambda}{f\overline{u}_A} T'(x, y, t) \sin(\pi z/H_A)$$

$$G_2 = \frac{g}{\theta_o}\frac{H_A}{\pi}. \quad (29)$$

The signs of the meridional wind anomaly at the ground and hence the SLP anomaly depend on the unknown function V_o. If the rigid boundary conditions (16) are applied to the vertical velocity, then $V_o = W_o = 0$. The vertical velocity structure is somewhat counterintuitive, with sinking in heating regions and rising in cooling regions. This is required by the vorticity balance, the relation between vertical shear of v_A and heating, and the rigid boundary conditions. The surface wind is equatorward over warm SST and poleward over cold (Figs. 3b and 5). A low pressure anomaly lies downstream of warm SST, which is opposite to observations of all decadal modes.

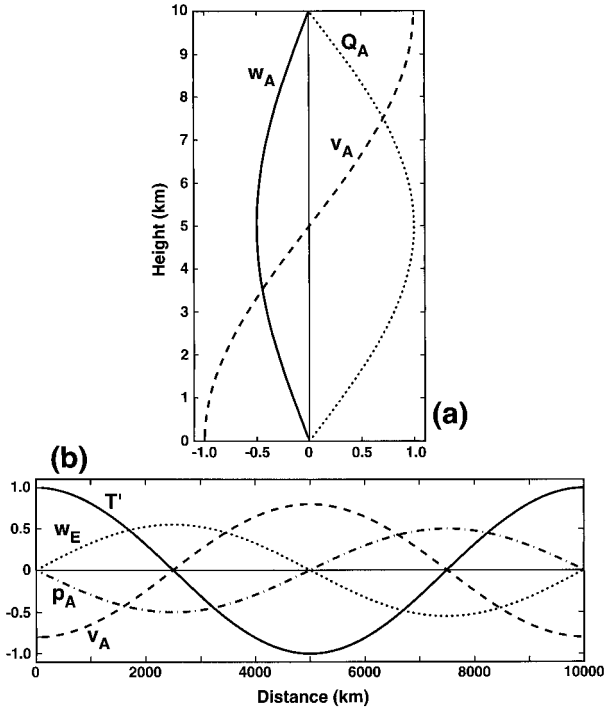

FIG. 5. Solution for zonal advection balancing heating in the atmosphere, with rigid upper and lower boundary conditions (16). This solution does not match any observed SST–SLP phasing. Units are arbitrary. (a) Heating Q_A, vertical velocity w_A, and meridional wind v_A with signs appropriate directly above a maximum positive SST anomaly. (b) Anomalies of SST T', SLP p_A, meridional surface wind v_A, and Ekman pumping w_E. Positive w_E (upwelling) cools SST directly, while poleward Sverdrup flow in the same location warms SST.

1) OCEAN HEAT CONVERGENCE RESPONSE (TABLE 2, COLUMN 2, ROW 1)

If the ocean response to the meridional wind anomaly is through Ekman heat convergence only, then from (4) and (10)

$$w_E = -G_2 \frac{\lambda}{\rho_o f^2 \overline{u}_A \delta}\frac{\partial T'}{\partial x}$$

$$\frac{\partial T'}{\partial t} + (\overline{u} + u_{ez})\frac{\partial T'}{\partial x} = -\kappa T'$$

$$u_{ez} \equiv -G_2 \frac{\gamma}{\rho_o \delta}\frac{\lambda}{f^2 \overline{u}_A}, \quad (30)$$

where u_{ez} is negative definite. A zonally periodic solution is

$$T' = T_o e^{-\kappa t}\cos\{k[x - (\overline{u} + u_{ez})t]\} \quad (31a)$$

$$v_A(z=0) = -G_2\frac{\lambda}{f\overline{u}_A}T_o e^{-\kappa t}\cos\{k[x - (\overline{u} + u_{ez})t]\} \quad (31b)$$

$$p_A(z=0) = -G_2\frac{\rho_A\lambda}{f\overline{u}_A k}T_o e^{-\kappa t}\sin\{k[x - (\overline{u} + u_{ez})t]\}. \quad (31c)$$

The atmosphere pressure anomaly is low east of warm SST. Under the low SLP, Ekman upwelling causes cooling, which therefore results in westward propagation at speed u_{ez} relative to the mean ocean flow. The meridional winds are strongest directly over the anomalies because the zonal atmospheric temperature gradient must be largest there.

2) Ocean Sverdrup response (Table 2, column 2, row 3)

If the ocean's Sverdrup response to Ekman pumping advects the background meridional temperature gradient $d\overline{T}/dy$, then

$$\frac{\partial T'}{\partial t} + (\overline{u} + u_{sz})\frac{\partial T'}{\partial x} = -\kappa T'$$

$$u_{sz} \equiv -G_2\frac{\lambda}{f\overline{u}_A}\frac{1}{\rho_o\delta\beta h_s}\frac{d\overline{T}}{dy}. \quad (32)$$

The solution for T', v_A, and p_A is identical to (31) with u_{ez} replaced by u_{sz}. East of a warm SST anomaly, SLP is low, there is Ekman upwelling, and poleward Sverdrup advection of warm water. Therefore the warm anomaly propagates eastward.

3) Equivalent barotropic atmosphere (Table 2, column 3)

Can zonal advection in the atmosphere lead to the correct spatial relation between SST and SLP anomalies? Qiu and Jin (1997) assumed an equivalent barotropic response in the atmosphere, which they assumed to be dominated by zonal advection. They did not apply the rigid boundary conditions. If a rigid lid is not imposed at $z = H_A$ and we make an ad hoc choice of V_0 in (29) such that the meridional wind is in the same direction at all heights and increases upward, for example,

$$V_o(x, y, t) = (\varepsilon_1 + G_2\lambda)\frac{1}{f\overline{u}_A}T'(x, y, t), \quad (33)$$

where ε_1 is a positive constant with units $m^2\ s^{-3}\ K^{-1}$, then the surface wind is poleward over warm SST and high SLP lies to the east of warm SST (Figs. 3a and 6), as observed. The opposite is true if the zonal wind anomaly is chosen to be minimum at the top and maximum at the ground. Assuming Ekman heat convergence (Table 2, column 3, row 1) rather than Sverdrup response in the ocean, the surface wind anomaly, the ocean Ekman pumping, and the SST anomaly equation are

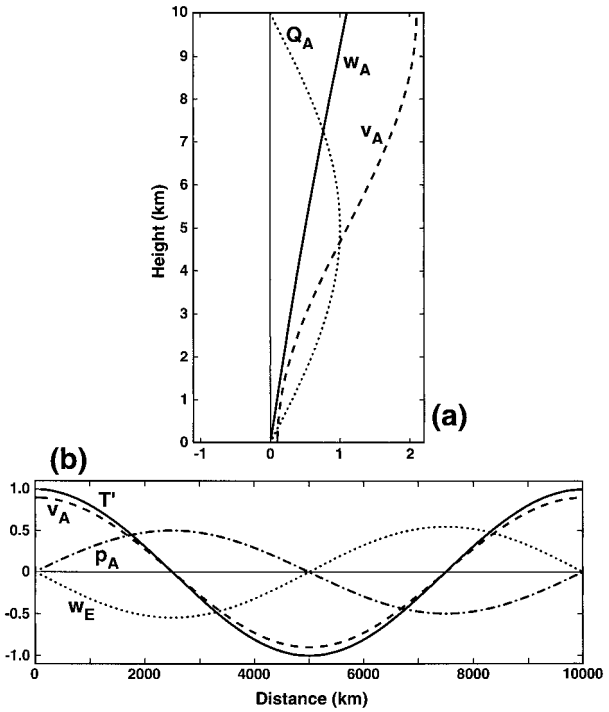

FIG. 6. Solution for zonal advection balancing heating in the atmosphere, with an ad hoc equivalent barotropic assumption with velocity of the same sign increasing upward. This produces the correct spatial phase for the ACW, North Pacific decadal, and North Atlantic interannual modes but requires a nonrigid vertical velocity boundary condition at the tropopause. Units are arbitrary. (a) Heating Q_A, vertical velocity w_A, and meridional wind v_A with signs appropriate directly above a maximum positive SST anomaly. (b) Anomalies of SST T', SLP p_A, meridional surface wind v_A, and Ekman pumping w_E. Positive w_E (upwelling) cools SST directly, while poleward Sverdrup flow in the same location warms SST.

$$v_A(z = 0) = \frac{\varepsilon_1}{f\overline{u}_A}T' \quad (34a)$$

$$w_E = \frac{\varepsilon_1}{\rho_o f^2\overline{u}_A\delta}\frac{\partial T'}{\partial x} \quad (34b)$$

$$\frac{\partial T'}{\partial t} + (\overline{u} + u_{ezbt})\frac{\partial T'}{\partial x} = -\kappa T', \quad (34c)$$

where the propagation speed relative to the mean ocean flow

$$u_{ezbt} = \frac{\gamma\varepsilon_1}{\rho_o\delta f^2\overline{u}_A}$$

is positive definite. A wave solution is

$$T' = T_o e^{-\kappa t} \cos\{k[x - (\overline{u} + u_{ezbt})t]\} \quad (35a)$$

$$v_A(z=0) = \frac{\varepsilon_1}{f\overline{u}_A} T_o e^{-\kappa t} \cos\{k[x - (\overline{u} + u_{ezbt})t]\} \quad (35b)$$

$$p_A(z=0) = \rho_A \frac{\varepsilon_1}{\overline{u}_A k} T_o e^{-\kappa t} \sin\{k[x - (\overline{u} + u_{ezbt})t]\}. \quad (35c)$$

The anomaly propagates eastward faster than the mean ocean flow. This enhancement results from the Ekman pumping response to meridional wind anomalies (and not from the mean zonal wind). The meridional winds are strongest directly over the SST anomalies because of the mean zonal wind, which moves the atmosphere's temperature anomaly downstream of the SST anomaly. With this ad hoc equivalent barotropic choice for v_A, high surface pressure is found east of warm SST, as observed; this is also true at all heights in the troposphere, with wind anomalies increasing with increasing height. If instead the surface wind had been chosen to be westward, reducing to zero wind at the tropopause, then low surface pressure would be found east of warm SST.

If an ocean Sverdrup advective response is assumed in this ad hoc equivalent barotropic model and ocean surface fluxes are included (Table 2, column 3, row 3), the solution is identical to (35), with u_{ezbt} replaced by

$$u_{szbt} = \frac{\varepsilon_1}{\rho_o f \overline{u}_A \beta \delta h_s} \frac{d\overline{T}}{dy}$$

$$v_g = \frac{\varepsilon_1}{\rho_o f^2 \overline{u}_A \beta \delta h_s} k T_o e^{-\kappa t} \sin\{k[x - (\overline{u} + u_{szbt})t]\}, \quad (36a\text{–}b)$$

where v_g is the meridional Sverdrup surface flow. Since $d\overline{T}/dy$ and f are of opposite sign in both hemispheres, u_{szbt} is negative. For this solution a high SLP east of warm SST causes Ekman pumping and equatorward Sverdrup flow of cold water. This results in westward propagation of the mode.

In this subsection we have seen that the SLP–SST phase relation depends again on the dominant atmospheric response, whereas the direction of propagation depends on the ocean response (since the time dependence is in the ocean temperature evolution). With rigid boundaries at the ground and tropopause, a low SLP anomaly is found east of high SST. Smagorinsky (1953) used the same rigid boundary conditions and his solutions, which include all of the terms together in the temperature equations, show such a response, suggesting that zonal advection in the atmosphere is an important part of his overall solution. The meridional wind anomaly reverses at midtroposphere and the solution is baroclinic. However, the observed interannual/decadal modes have high SLP east of warm SST and an equivalent barotropic atmosphere. If the latter assumption is made and the boundary conditions on vertical velocity are disregarded, then it is possible to find a zonal advective solution that matches the observations.

d. Atmosphere: Meridional advection balancing heating

A third two-term choice from the atmosphere's temperature equation (13) is between meridional advection of the mean meridional temperature gradient and heating:

$$v_A \frac{d\overline{\theta}}{dy} = Q_A(x, y, z, t). \quad (37)$$

Using (15) for Q_A and the vorticity equation (12), we obtain

$$v_A = \frac{\lambda}{d\overline{\theta}/dy} T'(x, y, t) \sin(\pi z/H_A)$$

$$w_A = W_o - \frac{\beta\lambda}{f d\overline{\theta}/dy} \frac{H_A}{\pi} T' \cos(\pi z/H_A). \quad (38)$$

This two-term balance is not well posed since it is not possible to apply both boundary conditions (16) for w_A with only one unknown. Because the mean temperature decreases toward the poles, this balance produces equatorward winds, bringing cold air into heating regions and poleward winds over cooling regions, which is the opposite from the observations. Also note that for this form (15) of Q_A, the wind is zero at the ground, although it might be reasonable to assume that for a less idealized choice, the wind could be in the same direction at the ground as at all other heights. Finally, much of this term in a full model could be canceled by a portion of the zonal advection term. Thus for several reasons it appears unlikely that a dominant balance between the meridional advective atmosphere term and heating holds. The remainder of this solution is not presented here, and it is not included in Table 2.

e. Atmosphere: Relaxation to heating

A final two-term choice for the atmosphere's temperature equation (13) is between heating and damping:

$$0 = Q_A - r\theta'. \quad (39)$$

Of all solutions presented herein, this one appears to be the most appropriate for the North Atlantic decadal mode. The meridional wind anomaly from the thermal wind relation (9b) is then

$$\frac{\partial v_A}{\partial z} = \frac{g}{f\theta_o} \frac{1}{r} \frac{\partial Q_A}{\partial x}. \quad (40)$$

Using the sinusoidal form (15) for Q_A, (40) yields

$$v_A = V_o - G_2 \frac{\lambda}{fr} \frac{\partial T'}{\partial x} \cos(\pi z/H_A)$$

$$w_A = W_o + \frac{\beta}{f} V_o z - G_2 \frac{\beta\lambda}{f^2 r} \frac{H_A}{\pi} \frac{\partial T'}{\partial x} \sin(\pi z/H_A), \quad (41)$$

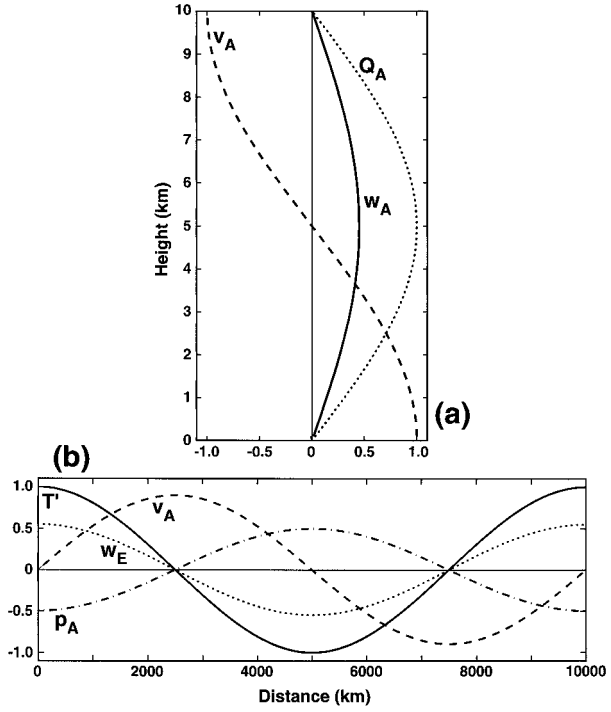

FIG. 7. Solution for relaxation to heating in the atmosphere. This solution produces the correct SST–SLP phasing for the North Atlantic decadal mode. Units are arbitrary. (a) Heating Q_A, vertical velocity w_A, and meridional wind v_A. The sign for Q_A is appropriate directly above the maximum positive SST anomaly, and signs for w_A and v_A are appropriate half a wavelength to the east [see (b) and Fig. 3c]. (b) Anomalies of SST T', SLP p_A, meridional surface wind v_A, and Ekman pumping w_E. Positive w_E (upwelling) cools SST directly, while poleward Sverdrup flow in the same location warms SST.

where T' is the surface temperature and the positive constant G_2 is defined in (29). The boundary conditions (16) yield $V_0 = W_0 = 0$. Here we find poleward wind east of warm SST and equatorward wind east of cold SST, hence low SLP over warm SST and high SLP over cold SST (Figs. 3c and 7). This is similar to Kushnir and Held's (1996) observation for a decadal North Atlantic mode.

1) OCEAN EKMAN HEAT CONVERGENCE (TABLE 2, COLUMN 4, ROW 1)

The equation for SST evolution (2) retaining the heat convergence term and including surface heat flux as well is

$$\frac{\partial T'}{\partial t} + \overline{u}\frac{\partial T'}{\partial x} = G_3\frac{\partial^2 T'}{\partial x^2} - \kappa T'$$

$$G_3 = \frac{G_2\lambda}{\rho_o f \delta r}\frac{\gamma}{f}, \tag{42}$$

where G_3 is positive. A zonally periodic solution to (41) and (42) is

$$T' = T_o e^{-\kappa_1 t}\cos[k(x - \overline{u}t)]$$

$$v_A = G_2\frac{\lambda}{fr}kT_o e^{-\kappa_1 t}\sin[k(x - \overline{u}t)]$$

$$p_A = -G_2\rho_A\frac{\lambda}{r}T_o e^{-\kappa_1 t}\cos[k(x - \overline{u}t)]$$

$$\kappa_1 = \kappa + G_3 k^2. \tag{43}$$

This mode is advected at the mean ocean flow speed. The ocean surface flux term (κ) damps the mode, as before. The atmosphere's relaxation response also causes decay due to the displacement of the meridional wind anomaly with respect to the SST anomaly, which means that the Ekman pumping anomaly is in phase with and reducing the SST anomaly. In section 3f it is seen that the additional decay term can be somewhat larger than the basic decay.

2) OCEAN SVERDRUP RESPONSE (TABLE 2, COLUMN 4, ROW 3)

If the ocean has a Sverdrup advection response to Ekman pumping, rather than mixed layer heat convergence, then (41) and (8) yield

$$\frac{\partial T'}{\partial t} + \overline{u}\frac{\partial T'}{\partial x} + G_4\frac{\partial^2 T'}{\partial x^2} = -\kappa T'$$

$$G_4 \equiv -\frac{G_2\lambda}{\rho_o f \delta r}\frac{1}{\beta h_s}\frac{dT}{dy}, \tag{44}$$

where G_4 is positive definite since the signs of the meridional temperature gradient and Coriolis parameter are opposite in each hemisphere. The solution is identical to (43) but with G_3 replaced by $-G_4$:

$$T' = T_o e^{-\kappa_2 t}\cos[k(x - \overline{u}t)]$$

$$\kappa_2 = \kappa - G_4 k^2. \tag{45}$$

Because the Sverdrup flow advects cold (warm) water into cold (warm) SST anomalies, this mode can grow if the advection effect is larger than the ocean heat flux damping—that is, if κ_2 is negative. This is the only complete solution presented in this paper that can grow without external forcing. In section 3f, the growth rate is evaluated and can be on the order of 100 days. Incomplete solutions for basins with western and eastern boundaries, presented in section 4, also have positive feedback and growth. If western and eastern boundaries were included with this solution, the western boundary current anomalies would create negative feedback, hence decay which could be offset by growth due to midbasin ocean Sverdrup response (45).

3) OCEAN SURFACE HEAT FLUX (DAMPING) (TABLE 2, COLUMN 4, ROW 2)

If the ocean temperature balance is (24), the solution is identical to (43) but with damping due to the ocean's

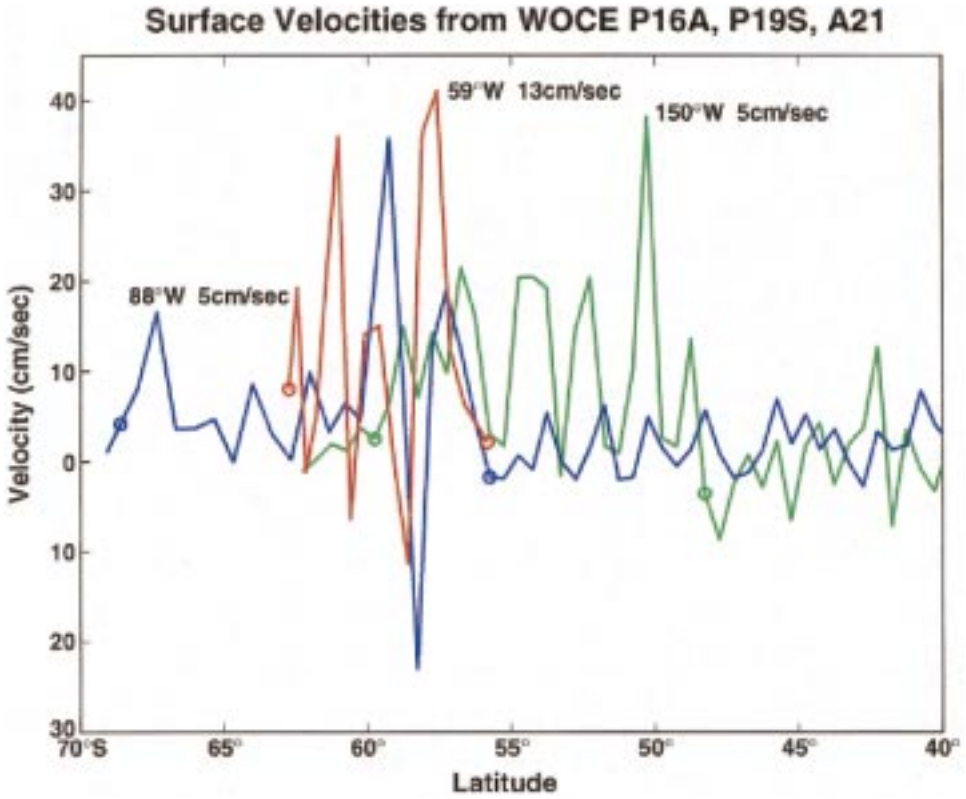

FIG. 8. Eastward geostrophic velocity at the sea surface relative to the ocean bottom, across the Antarctic Circumpolar Current (ACC) along 150°W (central Pacific), 88°W (eastern Pacific), and in Drake Passage, based on World Ocean Circulation Experiment sections P16, P19, and A21. The ACC is located between the heavy dots, based on water property changes (not shown). The mean eastward speed for the ACC for each section is given.

κ alone. Thus low SLP lies over high SST, with both the atmosphere and ocean temperatures responding passively to the heat flux from one to the other.

f. Phase speeds and timescales for zonally periodic solutions

Each of the solutions given above yields a phase speed for the coupled mode relative to the mean ocean flow. Since the purpose of these models is to understand a set of possible mechanisms through the simplest balances (in the usual sense of linear stability analyses), good correspondence between the predicted and observed propagation speeds should not be expected. The predicted propagation directions (west or east) are robust. The order of magnitude should be about right.

It is not clear what ''mean'' ocean zonal velocity is relevant for these relatively large-scale anomalies. The full latitude range of the eastward Antarctic Circumpolar Current includes two or three narrow bands of 30–50 cm s^{-1} embedded in much weaker eastward flow, as illustrated in Fig. 8 with several World Ocean Circulation Experiment hydrographic sections crossing the ACC in the Pacific from 150°W to Drake Passage. Peak speeds are 40 cm s^{-1} and mean speeds are 5–10 cm s^{-1}. The observed Antarctic circumpolar wave anomaly speed of 6–8 cm s^{-1} is of the same order as the average eastward flow speed and much lower than the peak frontal speeds, arguing for either stationarity or westward propagation of the mode relative to the mean ocean flow. Eastward flow in the North Atlantic and North Pacific currents is similarly banded.

Table 3 summarizes the phase speeds of the various zonally periodic modes based on parameter choices listed in Table 1. A latitude of 45° was chosen. All phase speeds are less than 20 cm s^{-1} and most are smaller than 5–10 cm s^{-1}, which is of the same order as the mean flow speed of the Antarctic Circumpolar Current (see section 3g below). The observed ACW and North Pacific SST–SLP spatial offset is produced by the models with vertical advection balancing heating in the atmosphere and with zonal advection balancing heating with an ad hoc equivalent barotropic assumption. With an ocean Sverdrup response, the ACW propagates westward for both of these models. Therefore the observed ACW propagation speed cannot be used to differentiate between these two models. Since the Sverdrup response produces westward propagation, it is the more likely oceanic mechanism than mixed layer heat convergence

response since the latter produces eastward phase speeds.

The balance that appears to dominate the North Atlantic decadal mode is local adjustment of the atmosphere's temperature to heating (relaxation). This mode propagates with the mean flow speed in these zonally periodic solutions and grows if a Sverdrup response is assumed in the ocean. The *e*-folding time for the mode (Table 3) is about 100 days for a 10 000-km wavelength, which is appropriate for the North Atlantic where the half-wavelength is about 5000 km.

g. Summary of zonally periodic solutions

Two scenarios for interannual to decadal midlatitude modes have been observed: 1) warm SST anomaly with high SLP anomaly lying to the east (ACW, North Pacific decadal mode, North Atlantic interannual mode), and 2) low SLP lying above warm SST (North Atlantic decadal mode) (references cited in the introduction). These behaviors can be produced through simple balances without resorting to the complications of instabilities or remote forcing.

The spatial relation of SST and SLP anomalies is given in the models by the dominant balance chosen for the atmosphere's temperature balance. Vertical advection (adiabatic heating) balancing diabatic heating and zonal advection of temperature anomalies balancing diabatic heating (with an ad hoc and hence troubling assumption of an equivalent barotropic atmosphere) both produce the observed SST–SLP offset for the first scenario. If the North Atlantic decadal mode were zonally periodic, then the most appropriate dominant balance would be relaxation of the atmosphere's temperature to local heating, as noted by Kushnir and Held (1996). This solution grows and so could maintain itself against damping.

The eastward phase speed of the modeled modes depends on choice of the ocean mechanism. Predicted phase speeds are within the range of the observed mode propagation speeds, which do not differ much from the mean flow speed. The one growing solution has an *e*-folding timescale of about 100 days, which is encouraging.

The vertical structure of the modes in the atmosphere is a potential diagnostic. However, the models here are so idealized that matching vertical structure is very tentative. Most are ''baroclinic'' in the sense of winds and SLP anomaly sign reversing in the upper troposphere relative to the lower. In the zonal advection/heating model, an equivalent barotropic structure (winds of same sign and increasing upward) had to be imposed to produce the observed SST–SLP relation, but it is not clear that the required disregard of boundary conditions is physically correct. W. White and S. -C. Chen (1997, personal communication) showed from observations that relative vorticity should not be neglected in the upper troposphere. When they included upper-troposphere relative vorticity in a model with a vertical advective/heating balance in the atmosphere, the observed coupled mode behavior at the ground was retained and, moreover, an equivalent barotropic atmosphere was produced.

Little is gained in this simple zonally periodic model by adding zonal channel boundaries or confining the anomalies to a limited meridional region. As mentioned above, the main addition to the solution would be meridional SST frontogenesis (formation of a zonal front) under high SLP and SST frontolysis under low SLP. These do not change the gross sense of location of the SST anomalies and SLP anomalies relative to each other.

The wavelength of the coupled mode is not determined by any of these solutions. It must be imposed externally or through the true, more complicated nonlinear dynamics including instability (e.g., Qiu and Jin 1997). One possibility is that the timescale is set by external forcing, such as propagation of the ENSO signal southward in the Pacific (Peterson and White 1998) or that the space scale is set externally [as invoked by Saravanan and McWilliams (1998)] perhaps through an intrinsic Pacific–South American mode (Christoph et al. 1998). The time and space scales are related through whatever dispersion relation is most applicable or the space scale is set by the basin scales in the Northern Hemisphere and by the two (Pacific and Atlantic/Indian) gyres of the Southern Hemisphere; then advection and Rossby wave propagation set the timescale (Latif and Barnett 1994; Cessi 1999).

4. Tendencies in bounded basins of the Northern Hemisphere

In the Northern Hemisphere the continental boundaries preclude the zonally periodic, propagating coupled mode described in section 3. Nevertheless, the decadal North Pacific and interannual North Atlantic modes show high (low) SLP centered east of warm (cold) SST, as in the circumpolar wave. Thus one might look to the vertical advective atmosphere and either Sverdrup or Ekman response in the ocean for basic balances in these modes. The North Atlantic decadal mode appears most like the atmosphere relaxation mode of section 3e, which also includes growth if an oceanic Sverdrup response is assumed.

What are some possible effects of boundaries on these modes? Negative feedback arises from increased transport of cold waters into the eastern subtropical gyre in the case of a warm SST anomaly in the west (Chelton and Davis 1982; Miller et al. 1994). These are subducted and advected around the gyre (Zhang and Levitus 1997; Deser et al. 1996). Westward baroclinic Rossby wave propagation also carries the uplifted thermocline signal from the eastern boundary (Latif and Barnett 1994; Jin 1997; Cessi 1999, among others). Both of these have timescales of more than a decade.

Short-term oceanic adjustment to the winds created

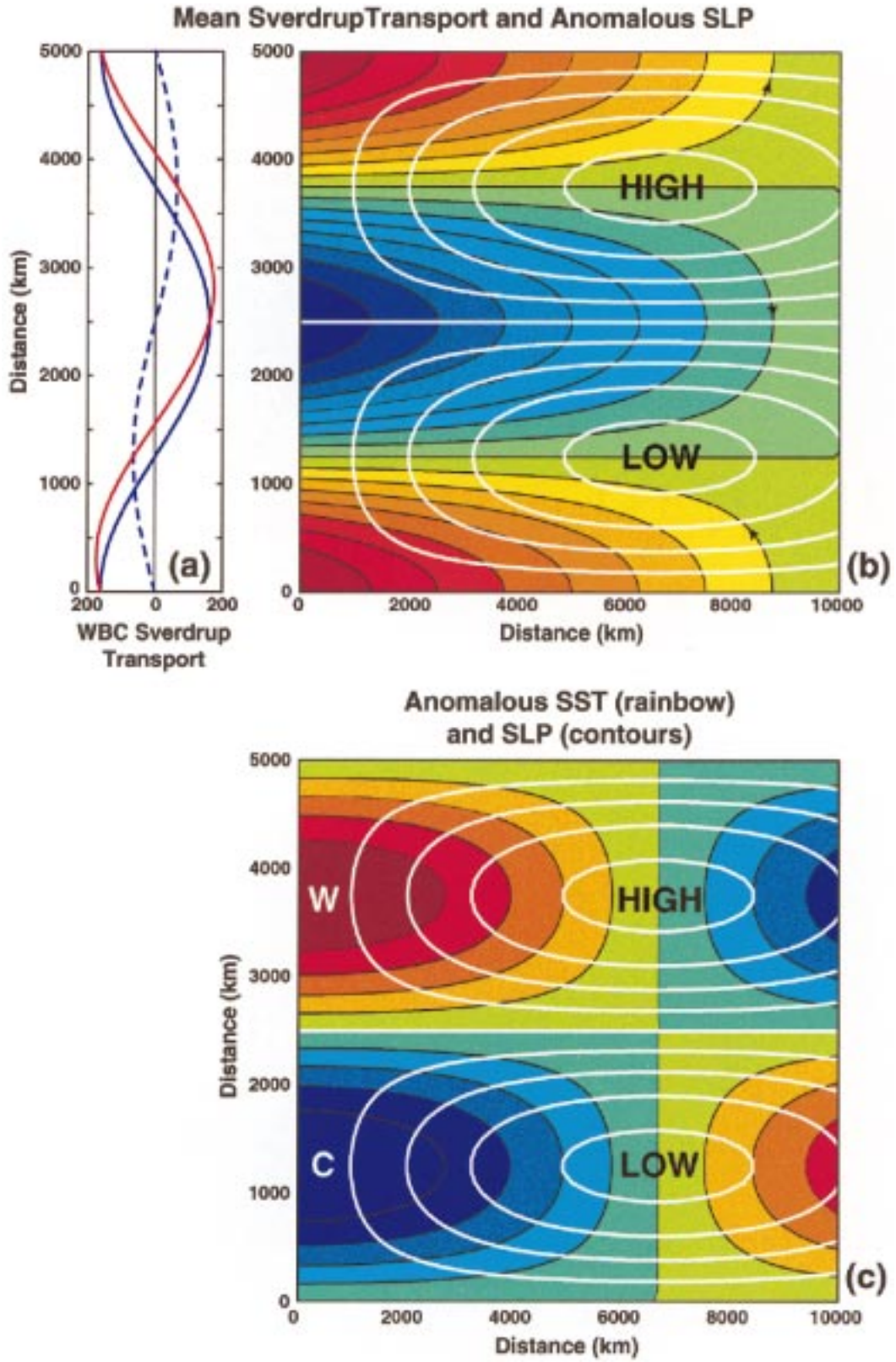

FIG. 9. Idealized bounded basin coupled mode assuming vertical advection balancing heating in the atmosphere. This solution is likely relevant for the North Pacific decadal mode. (a) Mean western boundary current transport (blue solid) based on mean Sverdrup transport. Anomalous western boundary current transport (blue dashed), assuming the SST

by anomalous SST can result in positive feedback, as described here. Barotropic adjustment of gyre transport to anomalous winds, with a timescale of one to two months for the North Pacific, could change the western boundary current strength and hence affect the anomalous SST in the western regions. Justification for short-term adjustment can be drawn from observations of the Oyashio strength relative to the Sverdrup transport of the North Pacific subpolar gyre (Sekine 1988; Hanawa 1995). The negative feedback leading to an oscillation would still be provided by the much longer baroclinic/advective adjustment as suggested by Latif and Barnett (1994).

The dominant pattern of SST anomaly in the North Pacific (e.g., Tanimoto et al. 1993) and its associated SLP anomaly is shown in schematic form in Fig. 1a. Consider here the Sverdrup transport anomaly associated with these anomalies and its effect on the western boundary current strengths. Assume the vertical advective atmosphere balance described in section 3b (column 1 in Table 2) since this produces the observed SST–SLP offset. An idealized mean circulation (Fig. 9b) is based on the observed zonally averaged wind stress curl; the western boundary current strength based on the mean idealized Sverdrup transport is shown in Fig. 9a. A simple sinusoidal SST pattern that mimics most of the observed SST anomaly features is used for ease of solution:

$$T' = T_o \cos(a\pi x/L_x) \sin(2\pi y/L_y); \qquad (46)$$

L_x and L_y are the zonal and meridional basin widths (10 000 km and 5000 km for the North Pacific in Fig. 9), and the factor a allows the western anomalies to extend eastward across the gyre (see Fig. 9c). For Fig. 9, a was chosen to be 0.75. The associated meridional wind anomaly is calculated from (18), the SLP anomaly from thermal wind (9), the geostrophic zonal wind anomaly from the SLP anomaly, and the Sverdrup transport anomaly from the meridional wind anomaly:

$$v_A(z = 0) = -\frac{f\lambda G_1}{\beta} T_o \cos(a\pi x/L_x) \sin(2\pi y/L_y)$$

$$\overline{\Psi}_{\mathrm{Sv}} + \Psi'_{\mathrm{Sv}} = \Psi_o(L_x - x) \cos(2\pi y/L_y) + \frac{f\lambda G_1}{\delta\beta^2} T_o \left(1 + \frac{4L_x^2}{a^2 L_y^2}\right) [\cos(a\pi x/L_x) - \cos(a\pi)] \sin(2\pi y/L_y), \qquad (47)$$

where Ψ_{Sv} is the Sverdrup transport streamfunction (mean and anomaly) and Ψ_o is the amplitude of the mean streamfunction. A warm SST anomaly ($T_o > 0$) leads to an increase in the subtropical gyre's western boundary current strength and a northward displacement of its separation latitude, based on Sverdrup transport (Fig. 9a). There is a concomitant weakening of the subpolar gyre's boundary current (Labrador Current/Oyashio). Thus a high SLP anomaly might bring more warm water into the western part of the gyre. This provides a positive feedback, strengthening the subtropical circulation further and enhancing the warm SST anomaly. Two associated positive feedbacks would also arise from the northward shift of the westerlies and storm track: reduced vertical mixing and reduced southward Ekman transport in the western boundary current separation region.

If the effect of surface heat fluxes on SST is considered, an enhanced high pressure reduces ocean heat loss in the western basin due to the increase in moisture-laden, warm winds there, while an enhanced low pressure increases ocean heat loss due to increase in cold, dry winds (Cayan 1992). These also create positive feedback with a short timescale.

For the decadal North Atlantic mode, for which the most likely mechanism of section 3 was relaxation of the atmosphere's temperature to the local heating, producing a low SLP over a warm SST, this type of barotropic adjustment reduces the basic SST anomaly. However, a growth mechanism in midbasin due to Sverdrup transport of the mean temperature gradient was described above in section 3e and could possibly maintain this mode against some damping and negative feedback.

5. Summary

The purpose of this work was to see what can be learned about the observed relations between SST, SLP, and meridional wind stress anomalies through simple,

←

anomaly pattern shown in (c). Total western boundary current transport (red). Note that the Kuroshio transport is increased, the Oyashio transport decreased, and the separation point is shifted northward. (b) Mean Sverdrup transport (color: reds are positive and blues are negative) and anomalous SLP. (c) Anomalous SST (color) and associated anomalous SLP (white contours). Reds are positive (W) and blues are negative (C). In (b) and (c) the upper SLP central closed contour is a high and the lower closed contour is a low, associated with this SST anomaly pattern.

local atmosphere–ocean coupling. Scale analysis showed that the temporal evolution of the slow coupled modes is based in the ocean's temperature equation, as was also found by Neelin (1991) for slow equatorial coupled modes. The spatial relation between the ocean and atmosphere fields is determined by the atmosphere's temperature equation. Newtonian cooling in the ocean damps the mode in all cases, whereas the equivalent term in the atmosphere can result in either damping or growth depending on other processes present.

Based on these exercises and upper-ocean observations relevant to climate (Miller and Schneider 1998), a useful linear framework for the circumpolar wave and North Pacific decadal and North Atlantic interannual modes appears to be an ocean Sverdrup response acting on the ocean's mean meridional temperature gradient, coupled to an atmosphere that has a Sverdrup response to vertical advection. If the atmosphere is assumed to be equivalent barotropic with nonzero wind in the same direction at the ground as aloft, an assumption that requires disregarding a rigid vertical boundary condition at the tropopause, then advection of the atmospheric temperature anomalies by the mean zonal wind can also produce the desired result.

For the North Atlantic decadal mode, with low SLP lying above warm SST (Kushnir and Held 1996), the simple model with atmosphere temperature responding directly to local heating appears most appropriate. If the ocean responds through Sverdrup transport changes in midbasin, then a local positive feedback could be possible.

For the North Pacific decadal and North Atlantic interannual modes, positive feedback within the midlatitude subtropical/subpolar gyre is likely on a short timescale corresponding to barotropic adjustment of the circulation and western boundary current strength to the wind stress anomalies resulting from the anomalous SST. Other positive feedbacks arise from these wind anomalies as well. Negative feedback providing an oscillation is most likely through slow baroclinic or advective adjustment, as described in a number of previous works (e.g., Latif and Barnett 1994).

The analysis presented here is meant to complement and not replace the many analyses showing the importance of tropical forcing on the midlatitudes through teleconnections. For the models of section 3, which best correspond to the circumpolar wave, external forcing or local instability are required to maintain the anomalies in the face of dissipation. Karoly (1989) shows the wave train patterns from the tropical Pacific to the Southern Hemisphere, suggesting remote forcing of the latter. Peterson and White (1998) demonstrate that the circumpolar wave anomalies appear to be stronger in the Pacific than in the Atlantic and Indian Oceans and suggest that the El Niño signal arising in the western tropical Pacific propagates to the Southern Ocean through an atmospheric teleconnection, thus providing a potential ongoing forcing to sustain the anomalies. Christoph et al. (1998) suggest that the intrinsic midlatitude mode of the Southern Hemisphere (Pacific–South American pattern) is significant, although its own sources are not clear. Remote forcing is also operative and may be critical in the midlatitude Northern Hemisphere (Hoskins and Karoly 1981; Trenberth and Hurrell 1994; Lau and Nath 1996; Zhang et al. 1996).

These simple models were presented in the same sense as linear stability analyses. The mechanisms revealed in them are robust, but likely not comprehensive due to the lack of more complicated wave dynamics, stochastic forcing, nonlinearity, remote forcing, and upper-ocean stratification/subduction. Some of these are included in work by the models of Jin (1997), Qiu and Jin (1997), and Saravanan and McWilliams (1998) in which there are still major simplifications in the physics. All of these simplified treatments allow greater understanding of the numerical models that are most often used, but whose complexity may make difficult the identification of simple mechanisms at the heart of the coupled modes.

Acknowledgments. This work was catalyzed by lectures by W. White and R. Peterson, who were helpful in initial discussions of the model. The reviewers' comments, which led to significant expansion of the work, are gratefully acknowledged. The work was supported through the NOAA Joint Institute for Marine Observations Consortium for Climate Research.

REFERENCES

Cayan, D. R., 1992: Latent and sensible heat flux anomalies over the northern oceans: Driving the sea surface temperature. *J. Phys. Oceanogr.,* **22,** 859–881.

Cessi, P., 1999: Thermal feedback on wind stress as a contributing cause of cimate variability. *J. Climate,* in press.

Chelton, D. B., and R. E. Davis, 1982: Monthly mean sea-level variability along the west coast of North America. *J. Phys. Oceanogr.,* **12,** 757–784.

Christoph, M., T. P. Barnett, and E. Roeckner, 1998: The Antarctic Circumpolar Wave in a coupled ocean–atmosphere GCM. *J. Climate,* **11,** 1659–1672.

Clement, A. C., R. Seager, M. A. Cane, and S. E. Zebiak, 1996: An ocean dynamical thermostat. *J. Climate,* **9,** 2190–2196.

Davis, R. E., 1976: Predictability of sea level pressure anomalies over the North Pacific Ocean. *J. Phys. Oceanogr.,* **8,** 233–246.

Deser, C., and M. L. Blackmon, 1995: On the relationship between tropical and North Pacific sea surface temperature variations. *J. Climate,* **8,** 1677–1680.

——, J. A. Alexander, and M. S. Timlin, 1996: Upper ocean thermal variations in the North Pacific during 1970–1991. *J. Climate,* **9,** 1840–1855.

Gill, A. E., 1980: Some simple solutions for heat-induced tropical circulations. *Quart. J. Roy. Meteor. Soc.,* **106,** 447–462.

Graham, N. E., T. P. Barnett, R. Wilde, U. Schlese, and L. Bengtsson, 1994: On the roles of tropical and midlatitude SSTs in forcing interannual to interdecadal variability in the winter Northern Hemisphere circulation. *J. Climate,* **7,** 1416–1441.

Hanawa, K., 1995: Southward penetration of the Oyashio water system and the wintertime condition of midlatitude westerlies over the North Pacific. *Bull. Hokkaido Natl. Fish. Res. Inst.,* **59,** 103–120.

Hoskins, B. J., and D. J. Karoly, 1981: The steady linear response of a spherical atmosphere to thermal and orographic forcing. *J. Atmos. Sci.,* **38,** 1179–1196.

Jin, F.-F., 1997: A theory of interdecadal climate variability of the North Pacific ocean–atmosphere system. *J. Climate,* **10,** 1821–1835.

Karoly, D. J., 1989: Southern Hemisphere circulation features associated with El Nino–Southern Oscillation events. *J. Climate,* **2,** 1239–1252.

Kushnir, Y., 1994: Interdecadal variations in North Atlantic sea surface temperature and associated atmospheric conditions. *J. Climate,* **7,** 141–157.

——, and I. M. Held, 1996: Equilibrium atmospheric response to North Atlantic SST anomalies. *J. Climate,* **9,** 1208–1220.

Latif, M., and T. P. Barnett, 1994: Causes of decadal climate variability over the North Pacific and North America. *Science,* **266,** 634–637.

——, and ——, 1996: Decadal climate variability over the North Pacific and North America: Dynamics and predictability. *J. Climate,* **9,** 2407–2423.

Lau, N.-C., and M. J. Nath, 1996: The role of the ''atmospheric bridge'' in linking tropical Pacific ENSO events to extratropical SST anomalies. *J. Climate,* **9,** 2036–2057.

Liu, Z., 1993: Interannual positive feedbacks in a simple extratropical air–sea coupling system. *J. Atmos. Sci.,* **50,** 3022–3028.

Miller, A. J., and N. Schneider, 1998: Interpreting the observed patterns of Pacific Ocean decadal variations. *Biotic Impacts of Extratropical Climate Change in the Pacific. Aha Huliko'a Hawaiian Winter Workshop,* University of Hawaii, Honolulu, HI, 19–27.

——, D. R. Cayan, T. P. Barnett, N. E. Graham, and J. M. Oberhuber, 1994: Interdecadal variability of the Pacific Ocean: Model response to observed heat flux and wind stress anomalies. *Climate Dyn.,* **9,** 287–302.

Mo, K. C., and G. H. White, 1985: Teleconnections in the Southern Hemisphere. *Mon. Wea. Rev.,* **113,** 22–37.

Namias, J., X. Yuan, and D. R. Cayan, 1988: Persistence of North Pacific sea surface temperature and atmospheric flow patterns. *J. Climate,* **1,** 682–703.

Neelin, J. D., 1991: The slow sea surface temperature mode and the fast-wave limit: Analytic theory for tropical interannual oscillations and experiments in a hybrid coupled model. *J. Atmos. Sci.,* **48,** 584–606.

Palmer, T. N., and Z. Sun, 1985: A modelling and observational study of the relationship between sea surface temperature in the northwest Atlantic and the atmospheric general circulation. *Quart. J. Roy. Meteor. Soc.,* **111,** 947–975.

Pedlosky, J., 1975: The development of thermal anomalies in a coupled ocean–atmosphere model. *J. Atmos. Sci.,* **32,** 1501–1514.

Peterson, R. G., and W. B. White, 1998: Slow oceanic teleconnections linking the Antarctic Circumpolar Wave with tropical ENSO. *J. Geophys. Res.,* **103,** 24 573–24 583.

Pitcher, E. J., M. L. Blackmon, G. T. Bates, and S. Munoz, 1988: The effect of North Pacific sea surface temperature anomalies on the January climate of a general circulation model. *J. Atmos. Sci.,* **45,** 173–188.

Qiu, B., and F.-F. Jin, 1997: Antarctic circumpolar waves: An indication of ocean–atmosphere coupling in the extratropics. *Geophys. Res. Lett.,* **24,** 2585–2588.

Roden, G. I., and J. L. Reid, 1961: Sea surface temperature, radiation and wind anomalies in the North Pacific Ocean. *Rec. Oceanogr. Works Japan,* **6,** 36–52.

Saravanan, R., and J. C. McWilliams, 1998: Advective ocean–atmosphere interaction: An analytical stochastic model with implications for decadal variability. *J. Climate,* **11,** 165–188.

Schneider, N., A. J. Miller, M. A. Alexander, and C Deser, 1999: Subduction of decadal North Pacific temperature anomalies: Observations and dynamics. *J. Phys. Oceanogr.,* **29,** 1056–1070.

Sekine, Y., 1988: Anomalous southward intrusion of the Oyashio east of Japan. 1: Influence of the seasonal and interannual variation in the wind stress over the North Pacific. *J. Geophys. Res.,* **93,** 2237–2255.

Smagorinsky, J., 1953: the dynamical influence of large-scale heat sources and sinks on the quasistationary mean motions of the atmosphere. *Quart. J. Roy. Meteor. Soc.,* **79,** 342–366.

Tanimoto, Y., N. Iwasaka, K. Hanawa, and Y. Toba, 1993: Characteristic variations of sea surface temperature with multiple time scales in the North Pacific. *J. Climate,* **6,** 1153–1160.

Trenberth, K. E., and J. W. Hurrell, 1994: Decadal atmosphere–ocean variations in the Pacific. *Climate Dyn.,* **9,** 303–319.

Tyrell, G. C., and D. J. Karoly, 1996: Links between tropical convection and variations of the extratropical circulation during TOGA COARE. *J. Atmos. Sci.,* **53,** 2735–2748.

VanScoy, K. A., and E. R. M. Druffel, 1993: Ventilation and transport of thermocline and intermediate waters in the northeast Pacific during recent El Niños. *J. Geophys. Res.,* **98,** 18 083–18 088.

White, W. B., and R. G. Peterson, 1996: An Antarctic circumpolar wave in surface pressure, wind, temperature, and sea ice extent. *Nature,* **380,** 699–702.

——, S.-C. Chen, and R. Peterson, 1998: The Antarctic Circumpolar Wave: A beta effect in ocean–atmosphere coupling over the Southern Ocean. *J. Phys. Oceanogr.,* **28,** 2345–2361.

Zebiak, S. E., and M. A. Cane, 1987: A model El Niño–Southern Oscillation. *Mon. Wea. Rev.,* **115,** 2262–2278.

Zhang, R.-H., and S. Levitus, 1997: Structure and cycle of decadal variability of upper ocean temperature in the North Pacific. *J. Climate,* **10,** 710–727.

Zhang, Y., J. M. Wallace, and N. Iwasaka, 1996: Is climate variability over the North Pacific a linear response to ENSO? *J. Climate,* **9,** 1468–1478.